NMRF/VR/01/2024

VERIFICATION REPORT

NCUM Global Model Verification: October-November 2023

K. NIRANJAN KUMAR, SUKHWINDER KAUR, MOHANA S. THOTA, M. VENKATARAMI REDDY, HARVIR SINGH, SUSHANT KUMAR, ANUMEHA DUBE, SUMIT KUMAR, RAGHAVENDRA ASHRIT, SAJI MOHANDAS, & V S PRASAD

Feb 2024

National Centre for Medium Range Weather Forecasting
Ministry of Earth Sciences, Government of India
A-50, Sector-62, NOIDA-201 309, INDIA

NCUM Global Model Verification:
October-November 2023

K. NIRANJAN KUMAR, SUKHWINDER KAUR, MOHANA S. THOTA, M. VENKATARAMI REDDY, HARVIR SINGH, SUSHANT KUMAR, ANUMEHA DUBE, SUMIT KUMAR, RAGHAVENDRA ASHRIT, SAJI MOHANDAS, & V S PRASAD

NMRF/VR/01/2024

National Centre for Medium Range Weather Forecasting
Ministry of Earth Sciences, Government of India
A-50, Sector 62, NOIDA-201309, INDIA
www.ncmrwf.gov.in

Data Control Sheet

1	Name of the Institute	National Center for Medium range weather Forecasting, MoES, India
2	Document Number	NMRF/VR/05/2023
3	Date of Publication	Feb 2024
4	Title of the document	NCUM Global Monthly Verification: October-November 2023
5	Type of the document	Verification Report
6	Number of pages, figures, and Tables	46 pages, 34 figures, and 4 Tables
7	Authors	K. Niranjan Kumar, Sukhwinder Kaur, Mohana S. Thota, M. Venkatarami Reddy, Harvir Singh, Sushant Kumar, Anumeha Dube, Sumit Kumar, and Raghavendra Ashrit, Saji Mohandas, & V S Prasad
8	Originating Unit	National Centre for Medium Range Weather Forecasting (NCMRWF), A-50, Sector-62, NOIDA201 309, India.
9	Abstract	This report documents the analysis and forecasting performance of the global NCMRWF Unified Model (NCUM-G) during the Northeast monsoon season (ON) 2023. The verification results are presented to address (a) forecasters and (b) model developers. The information on biases in the forecasted winds, temperature, humidity, rainfall, etc., are crucial for the forecasters to interpret the model guidance for accurate forecasting. Furthermore, details on recent enhancements in the model's skill contribute to strengthening confidence in the accuracy of the model forecasts.
10	References	15
11	Security classification	Unrestricted
12	Distribution	General

Table of Contents

S.No		P.No.
	Abstract	1
1	**Introduction**	2
2	**NCMRWF Unified Modelling System & Verification datasets**	2
	2.1. Model Description *2.2. Observed/analysis Data used for the verification*	
3	**NCUM-G Analysis Mean and Anomalies during ON 2023**	3
	3.1. Winds at 850, 700, 500, and 200 hPa levels *3.2. Temperature at 850, 700, 500, and 200 hPa levels* *3.3. Relative Humidity (RH) at 850, 700, and 500 hPa levels*	
4	**Systematic Errors in NCUM-G Forecasts**	10
	4.1. Winds at 850, 700, 500, and 200 hPa levels *4.2. Temperature and Relative Humidity* *4.3. Surface (10m) winds* *4.4. Temperature at 2m* *4.5. Total Precipitable Water (PWAT)*	
5	**Rainfall Forecast Verification during ON 2023**	25
	5.1. Mean and Mean Error *5.2. Categorical Scores of Rainfall Forecast* *5.3. Total Interest*	
6	**Significant Weather Events during Oct-Nov 2023**	30
	6.1. **Arabian Sea ESCS 'Tej' during 20-24 Oct 2023** ***6.1.1.*** *Forecast Tracks and Strike Probability* *6.1.2. Forecast Track Errors* *6.1.3. Forecast Intensity Errors (Min SLP and Max Wind)* *6.1.4. Forecast Landfall Error* *6.1.5. Verification of Strike Probability* ***6.2. Bay of Bengal VSCS 'Hamoon' during 21-25 Oct 2023*** *6.2.1. Forecast Tracks and Strike Probability* *6.2.2. Forecast Track Errors* *6.2.3. Forecast Intensity Errors (Min SLP and Max Wind)* *6.2.4. Forecast Landfall Error* 6.2.5. *Verification of Strike Probability*	
7	**Summary and Conclusions**	42
8	**References**	46

NCUM Global Model Verification: October-November 2023

K. Niranjan Kumar, Sukhwinder Kaur, Mohana S. Thota, M. Venkatarami Reddy, Harvir Singh, Sushant Kumar, Anumeha Dube, Sumit Kumar, Raghavendra Ashrit, Saji Mohandas, & V S Prasad

सारांश

यह रिपोर्ट पूर्वोत्तर मानसून सीजन (अक्टूबर-नवंबर) 2023 के दौरान वैश्विक रा.म.अ.मौ.पू.कें. यूनिफाइड मॉडल (एन.सी.यू.एम.-जी) के विश्लेषण और पूर्वानुमान प्रदर्शन का दस्तावेजीकरण करती है। सत्यापन परिणाम (ए) पूर्वानुमानकर्ताओं और (बी) मॉडल डेवलपर्स को संबोधित करने के लिए प्रस्तुत किए जाते हैं। सटीक पूर्वानुमान के लिए मॉडल मार्गदर्शन की व्याख्या करने के लिए पूर्वानुमानित हवाओं, तापमान, आर्द्रता, वर्षा आदि में पूर्वाग्रहों की जानकारी पूर्वानुमानकर्ताओं के लिए महत्वपूर्ण है। इसके अलावा, मॉडल के कौशल में हालिया संवर्द्धन का विवरण मॉडल पूर्वानुमानों की सटीकता में विश्वास बढ़ाने में योगदान देता है।

Abstract

This report documents the analysis and forecasting performance of the global NCMRWF Unified Model (NCUM-G) during the Northeast monsoon season (ON) 2023. The verification results are presented to address (a) forecasters and (b) model developers. The information on biases in the forecasted winds, temperature, humidity, rainfall, etc., are crucial for the forecasters to interpret the model guidance for accurate forecasting. Furthermore, details on recent enhancements in the model's skill contribute to strengthening confidence in the accuracy of the model forecasts.

1. Introduction

The performance of the global NCMRWF Unified Model (NCUM-G) forecasts during the October-November (ON) season of 2023 is presented in this report. The main aim of this assessment is to ascertain the accuracy and reliability of the forecasts through a comprehensive comparison with model analyses and observational data. The results are summarized for the post-monsoon season to understand the average biases and forecast performances. The report is oriented towards both (a) forecasters and (b) model developers. In section 2, the report outlines the NCUM-G model description and data assimilation system at NCMRWF along with detailing the observed data used in this report. Moving on to section 3, a thorough examination of the seasonal mean analysis and corresponding anomalies is presented, offering readers a comprehensive perspective on the model's performance throughout the northeast monsoon season. Section 4 of the report discusses the systematic biases observed in the forecasted large-scale upper fields such as wind, temperature, humidity, along with rainfall etc., which are expected to be useful for the forecasters to interpret the model forecasts effectively. Section 5 subsequently provides a careful validation of the forecasts. Section 6 is devoted to the verification of significant weather events during the ON 2023 season. This encompasses the verification of the NCMRWF model forecasts for the two systems: the Extremely Severe Cyclonic Storm (ESCS) “Tej” over Arabian Sea during 20-24 Oct 2023 and Very Severe Cyclonic Storm (VSCS) “Hamoon” over Bay of Bengal during 21-25 Oct 2023. Section 7 provides a concise summary of the obtained results.

2. NCMRWF Unified Modelling System & Verification datasets

2.1. Model Description

The NCMRWF started using the Unified Model (UM) Partnerships’ seamless prediction system since 2012, naming this system as NCUM. The NCUM global Numerical Weather Prediction (NWP) system (NCUM-G) became operational in 2012 with a grid resolution of 25km (NCUM-G:V1) designed for medium-range weather prediction. This system underwent successive upgrades, progressing to a 17 km horizontal resolution (NCUM-G:V3) in 2015, followed by a refinement to a 12km resolution (NCUM-G:V5) in 2018. Further enhancements were made in 2020, resulting in a 12 km resolution coupled with improved model physics (NCUM-G:V6). The present version (NCUM-G:V7) of NCUM-G has a horizontal grid resolution of ~12 km with 70 levels in the vertical reaching 80 km height. It uses “ENDGame” dynamical core, which provides improved accuracy of the solution of primitive model equations and reduced damping. This helps in producing finer details in the simulations of synoptic features such as cyclones, fronts, troughs, and jet stream winds. ENDGame also increases variability in the tropics, which leads to an improved representation of tropical cyclones and other tropical phenomena. The model uses improved physics options of GA7.2 (Walters et al., 2017). An advanced data assimilation method of Hybrid 4-Dimensional Variational (4D-Var) is used for the creation of NCUM global analysis. The advantage of the Hybrid 4D-Var is that it uses a blended background error, a blend of “climatological” background error, and day-to-day varying flow dependent background error (derived from the 22–member ensemble forecasts). The hybrid approach is scientifically attractive because it elegantly combines the benefits of ensemble data assimilation (flow-dependent co-variances) with the known benefits of 4D-Var within a single data assimilation system (Barker, 2011). A brief description of the NCUM Hybrid 4D-Var system is given in Kumar et al. (2021, 2020, & 2019).

2.2. Observed/analysis Data used for the Verification

The seasonal mean analysis and anomalies are studied using the fifth-generation European Centre for Medium-Range Weather Forecasts (ECMWF) reanalysis product (ERA-5) (Hershbach et al. 2020) climatology (1979-2018). The high resolution (12km) NCUM-G analysis data is interpolated to ERA-5 grid resolution (0.25^0x0.25^0). For verification of the forecasts, the NCUM-G model analysis is used. All systematic errors are computed at a native grid resolution of 12km.

Detailed quantitative rainfall forecast verification is based on the India Meteorological Department (IMD)-NCMRWF daily high resolution (0.25^0) rainfall analysis (Mitra et al. 2009, 2013). The rainfall analysis objectively analyses India Meteorological Department (IMD) daily rain gauge observations onto a 0.25^0 grid using a successive corrections technique with the GPM Satellite rainfall providing the first guess estimates. The model forecasts are gridded to the 0.25^0 observed rainfall grids over Indian land regions for 61 days from 1st October 2023 to 30th November 2023. The merging of the IMD gauge data into GPM estimates not only corrects the mean biases in the satellite estimates but also improves the large-scale spatial patterns in the satellite field, which is affected by temporal sampling errors (Mitra et al. 2009). Verification of daily temperature forecasts is carried out against the IMDs daily observed gridded (0.5^0 x 0.5^0) maximum (Tmax) and minimum (Tmin) temperature data (Srivastava et al. 2009).

3. NCUM-G Analysis Mean and Anomalies during ON 2023

3.1. Winds at 850, 700, 500, and 200 hPa levels

This section evaluates the NCUM-G analysis fields and deviations from the climatological norm for October and November 2023, focusing on wind patterns, temperature, and relative humidity at the standard atmospheric pressure levels of 850, 700, 500, and 200 hPa. These anomalies are calculated based on the ERA5 climatology for the period 1979-2018.

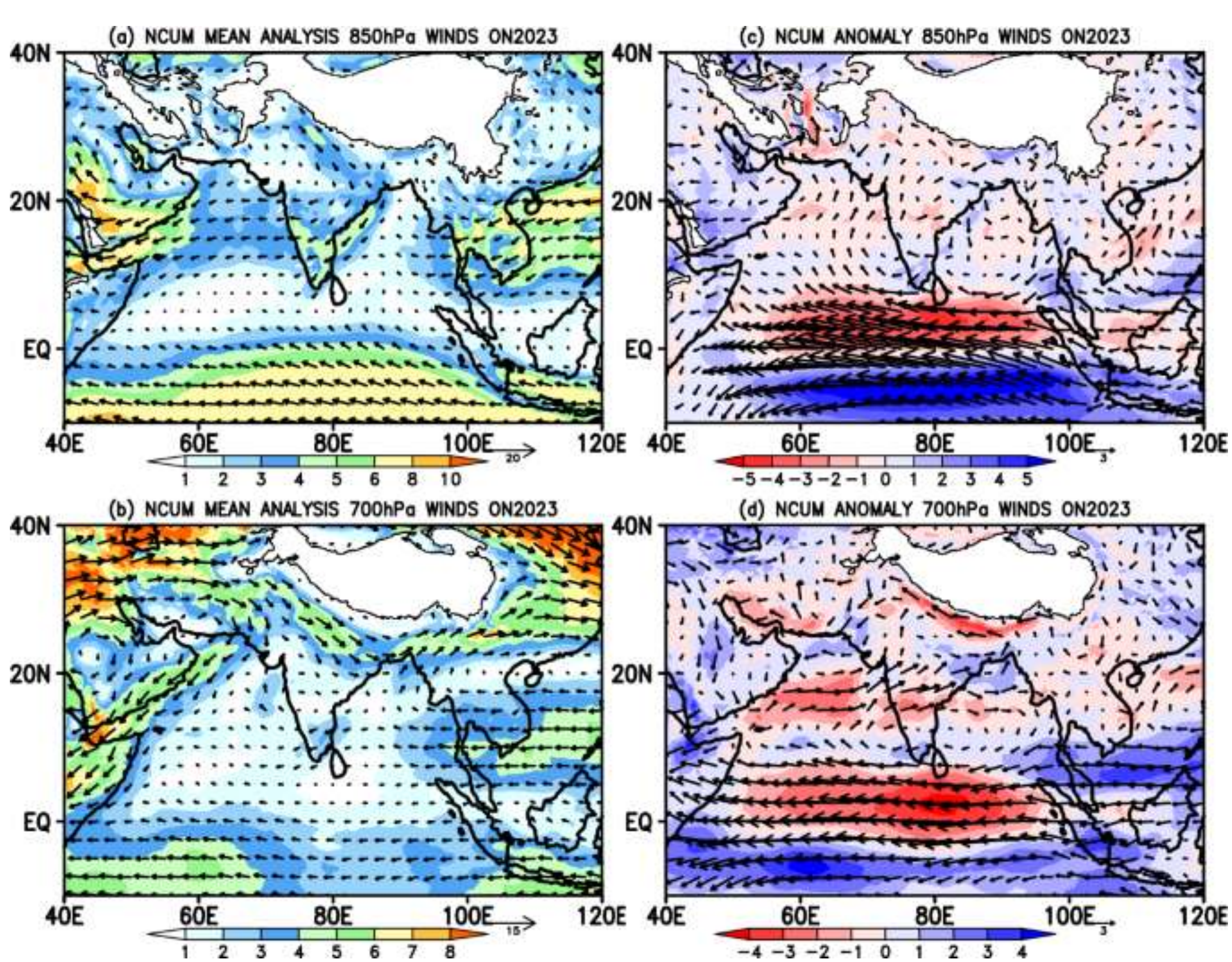

Figure 1. Mean winds at (a) 850 hPa and (b) 700 hPa in the NCUM-G Analysis during ON 2023 (m/s). Right panels show the anomaly circulations at (c) 850 hPa and (d) 700 hPa.

During the October-November 2023 season, notable climatic features include the shift in wind direction from the southwesterlies to northeasterlies across the Indian subcontinent, a departure from the usual summer winds observed from June through September. This period also saw significant rainfall in the southeastern part of peninsular India, marking it as a significant quasi-permanent climatic event (Rajeevan et al. 2012). The analysis initially focuses on the mean wind patterns and their anomalies at the 850 and 700 hPa levels as derived from the NCUM-G analysis, illustrated in Figures 1a-d.

At the 850 hPa level, the wind patterns during this season predominantly showed easterly to northeasterly directions towards southern peninsular India (Figure 1a), associated with the southward migration of the Inter Tropical Convergence Zone (ITCZ) and the formation of high-pressure systems over the Tibetan and Siberian Plateaus. A strong easterly to southeasterly flow was notably present south of the equatorial Indian Ocean.

At the 700 hPa level (Figure 1b), the mean wind patterns shared similarities with those at 850 hPa, with the addition of a pronounced northeasterly flow over the Horn of Africa and the adjacent Arabian Sea, which was not observed at the 850 hPa level. The wind anomalies for the October-November 2023 season, compared to the ERA5 climatology, are depicted in Figures 1c and 1d. At both 850 and 700 hPa levels, the NCUM-G analysis revealed strong anomalous easterlies over the equatorial Indian Ocean, relative to the ERA5 reanalysis. Over the Indian landmass, the analysis at 700 hPa highlighted significant anomalous southerlies, indicating a weakening of the usual northerly winds. Additionally, the wind anomaly maps indicate an anomalous anti-cyclonic circulation over the southern Bay of Bengal. Similar patterns of anomalous flow for the October-November 2023 season were observed at the 700 hPa level.

The mid- and upper- tropospheric (500 and 200 hPa) mean winds and corresponding anomalies from ERA5 climatology are shown in Figure 2. One of the main synoptic features is the subtropical westerlies between 20-40^{o}N with a westward moving series of troughs and ridges. At 500 hPa, the deflection of westerlies between 20-40^{o}N and 80-100^{o}E can be seen in the mean winds due to Himalayan topography. The strength of these westerlies has increased from 500 hPa to 200 hPa. The peak of the subtropical jet (STJ) is clearly visible/seen at 200 hPa (Figure 2b) with magnitudes more than 40m/s. At the same time over the southern region reduction in the strength of easterlies can be seen at 200 hPa level. Further, the associated anomalous wind flow for ON 2023 in the mid- and upper troposphere is presented in Figures 2c and 2d. The westerlies over south India are clearly observable, while, simultaneously, the magnitudes of winds in central and north India are higher than the climatology at 500hPa (Figure 2c). In the upper troposphere, the anomalous winds exhibit strong westerlies below 25^{o}N and easterlies above 25^{o}N, consequently inducing an anomalous cyclonic circulation clearly visible over the northern Indian region (Figure 2d). The tropical easterlies on the other hand indicate above (below) normal with magnitudes of about 5-6m/s at 500hPa (200hPa).

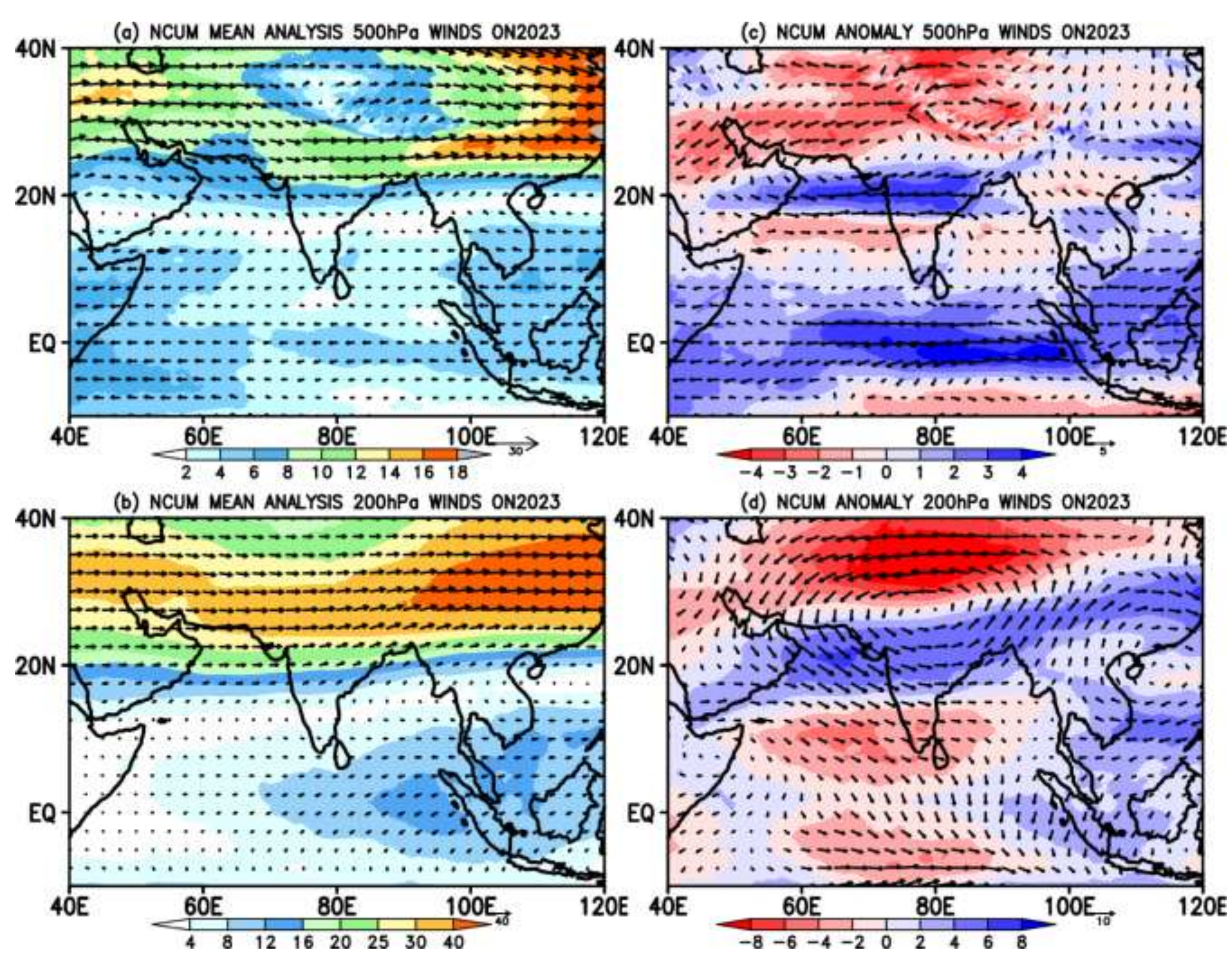

Figure 2. Mean winds at (a) 500 hPa and (b) 200 hPa in the NCUM-G Analysis during ON 2023 (m/s). Right panels show the anomaly circulations at (c) 500 hPa and (d) 200 hPa.

3.2. Temperature at 850, 700, 500, and 200 hPa levels

The spatial distribution of seasonal mean temperatures in the lower troposphere is shown in Figures 3a and 3b. The mean daily temperature at lower levels (i.e., at 850hPa) exceeds 19^0C over the north-western Indian regions (Figure 3a). In contrast to the temperatures at 850hPa level, the spatial map of temperature at 700 hPa is quite homogeneous ranging between 8-10^0C, except over some parts of the BoB. This relatively strong heating in the lower troposphere over oceanic regions probably enhances the low-levels convergence of winds and troughing and subsequently, the cyclogenesis noted earlier. The anomalous temperature distribution in the lower troposphere (i.e., at 850hPa and 700hPa) is indicated in Figures 3c and 3d. At 850hPa, positive anomalies ranging from 1-2^0C (depicted in red) are observable across the entire domain (Figure 3c). The above-normal temperature over BoB relative to climatological means with magnitudes of 2^0C is favorable for convective initiation over BoB. At 700 hPa, positive anomalies are widespread, except for the north-west parts of India (Figure 3d).

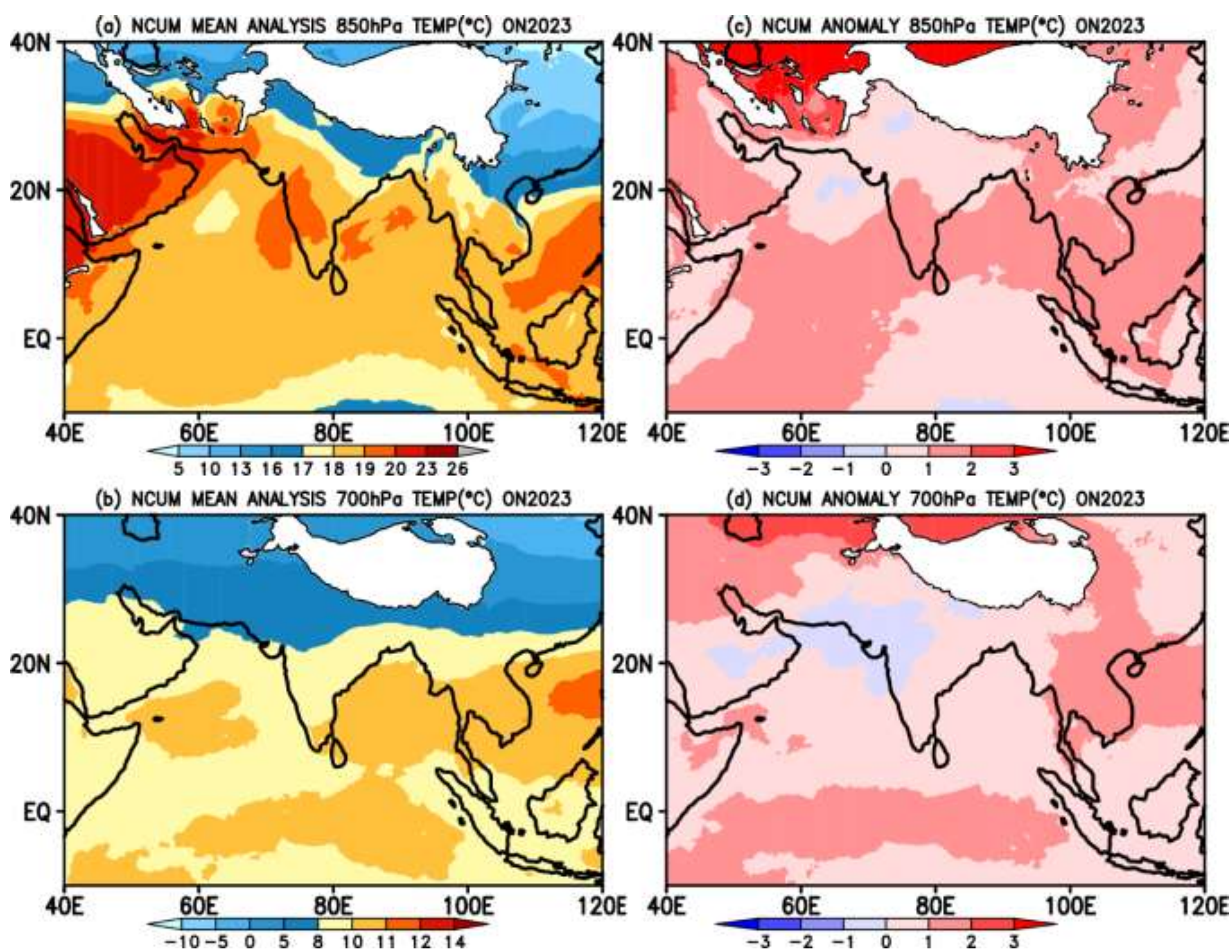

Figure 3. Mean Temperature (Degree Celsius, ^{0}C) at (a) 850 hPa and (b) 700 hPa in the NCUM-G Analysis during ON 2023. Right panels show the Temperature anomalies at (c) 850 hPa and (d) 700 hPa.

The spatial distribution of mid- and upper-tropospheric temperatures and corresponding anomalies with respect to the seasonal mean climatology is shown in Figure 4. The seasonal mean temperature at 500 hPa during ON 2023 indicates quite uniform over the Indian subcontinent and adjoining seas (Figure 4a). On the other hand, the anomalous features (Figures 4c and 4d) indicate the above-normal temperatures over almost the entire domain at 500 and 200hPa, excluding the region between 35-40^{o}N and 60-100^{o}E at 200 hPa.

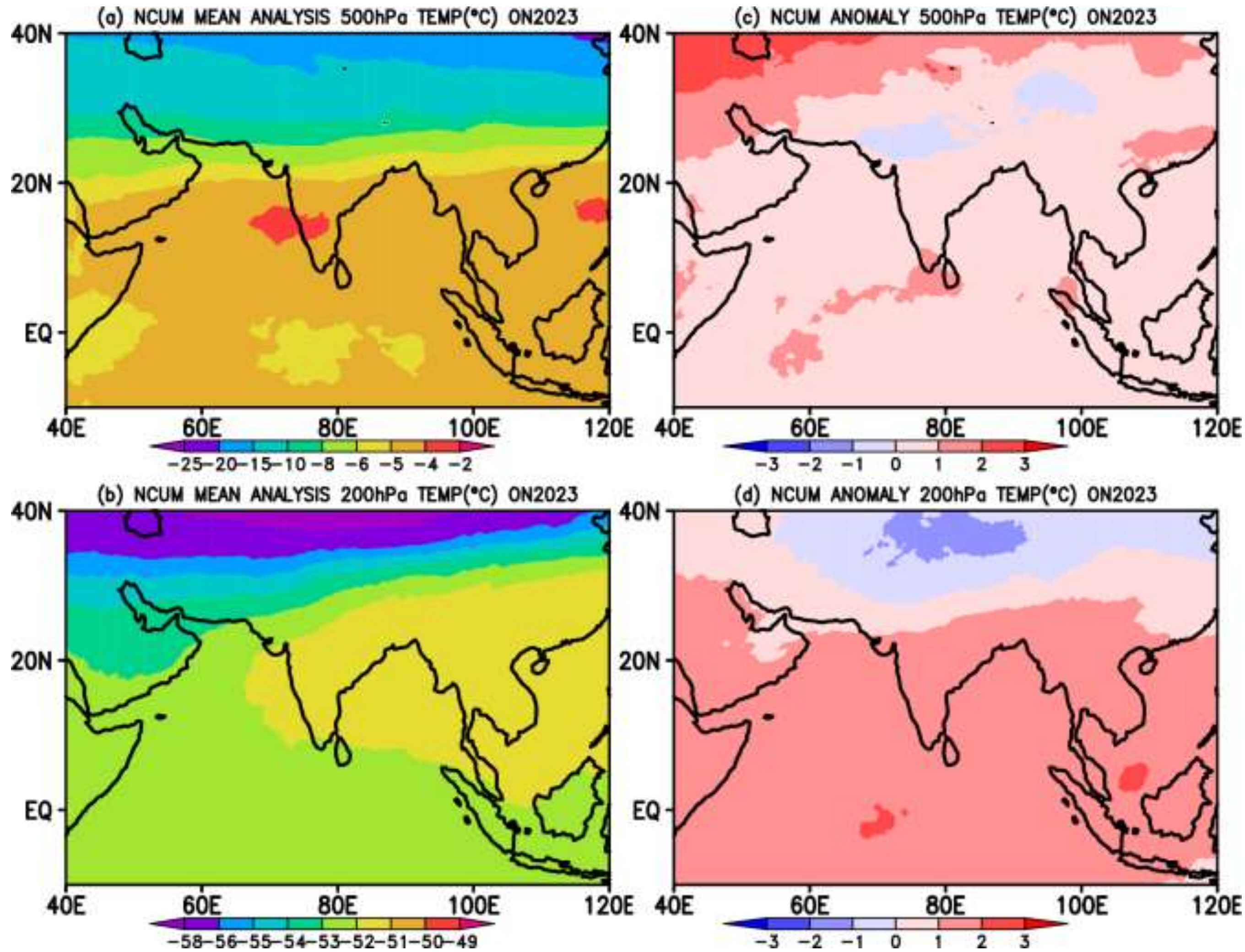

Figure 4. Mean Temperature (Degree Celsius, ^{0}C) at (a) 500 hPa and (b) 200 hPa in the NCUM-G Analysis during ON 2023. Right panels show the Temperature anomalies at (c) 500 hPa and (d) 200 hPa.

3.3. Relative Humidity (RH) at 850,700, and 500 hPa levels

The spatial distribution of humidity is an important field along with wind and temperature for its influence on the rainfall. In Figure 5, we showed the spatial distribution of seasonal mean humidity and consequent anomalies in the lower troposphere. It is clearly noticed from Figure 5a that the lower tropospheric humidity is larger over the southern peninsula India. This could be associated with the strong easterly flow from BoB to the Indian subcontinent during North-East Monsoon (NEM) and rainfall spells associated with the easterly waves. There is a significant amount of difference between the north and south of India w.r.t the magnitudes of RH at both 850 hPa and 700 hPa levels (Figures 5a and 5b). Also, the high humidity can be noticed over the equatorial Indian Ocean and Maritime Continent (MC). When we see the anomalous distribution for the ON 2023, the below-normal percentage of RH can be clearly visible over most of the Indian land region and neighboring seas excluding Arabian Sea (AS) and head BoB at 850 hPa. As we move to the 700 hPa level, we can see the decrease in RH over southern peninsular India (Figure 5b), consequently, the anomalies indicate the above-normal values over most of Indian land region and over the surrounding oceanic regions excluding eastern equatorial Indian Ocean during ON 2023 (Figure 5d). A similar spatial structure in RH at 500 hPa level is also noted in NCUM-G. Further, the RH anomalies indicate above normal over BoB and coastal regions around the south peninsular India (Figure 6b). Hence, this above-normal RH (see Figures 5 and 6) from lower to mid-troposphere contributes to delivering the excess rainfall amounts over BoB and southern peninsular India in NCUM-G, which will be seen in Section 5.

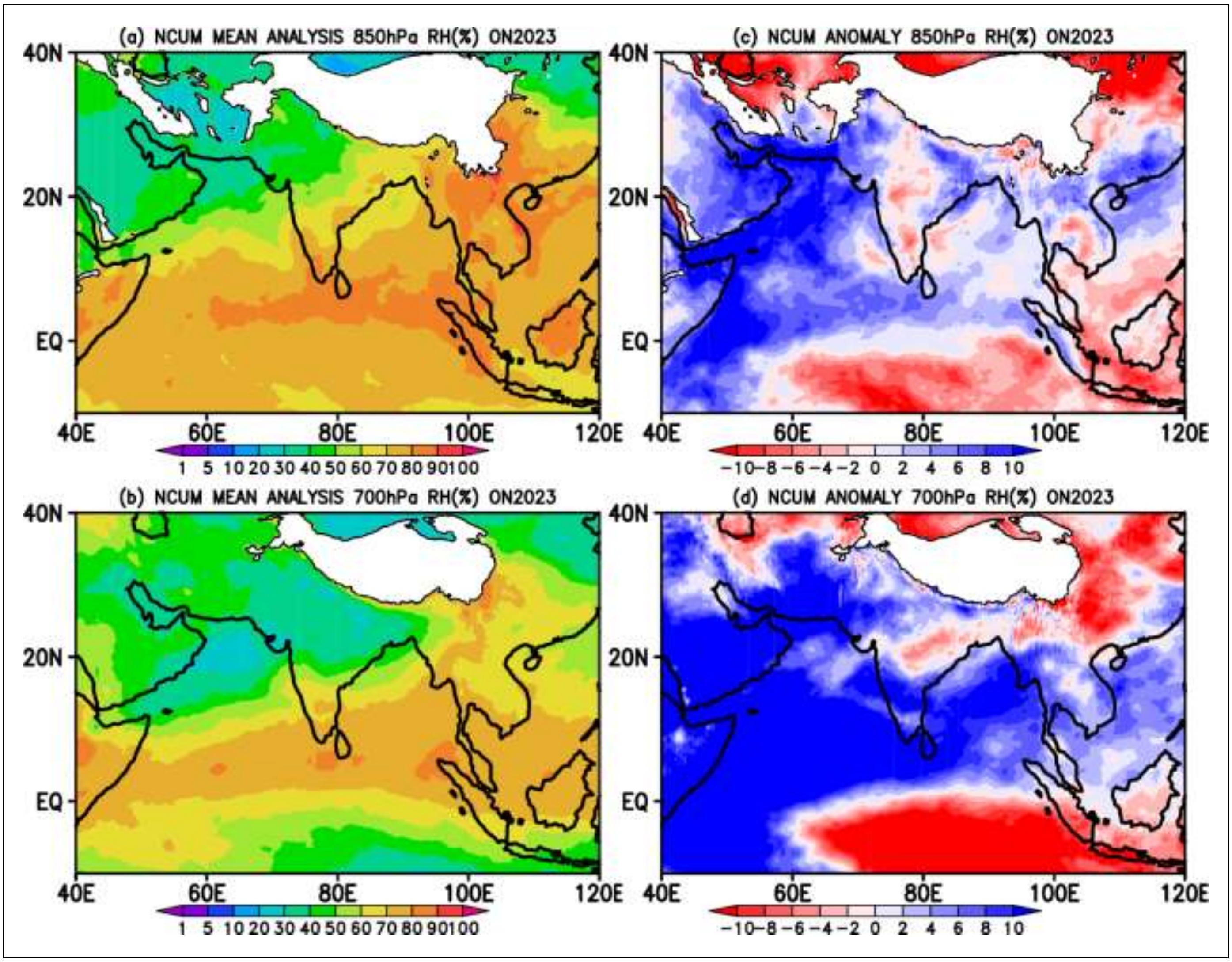

Figure 5. Mean Relative Humidity (%) at (a) 850 hPa and (b) 700 hPa in the NCUM-G Analysis during ON 2023. The right panels show the anomalies in Relative Humidity at (c) 850 hPa and (d) 700 hPa.

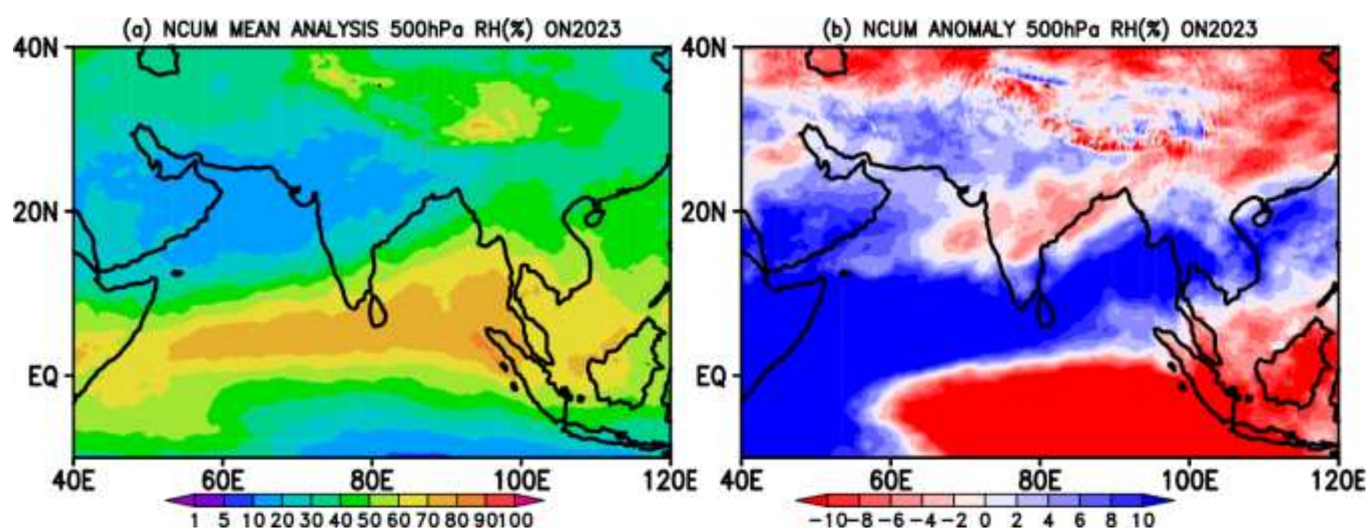

Figure 6. Mean Relative Humidity (%) (a) Mean and (b) anomaly at 500 hPa in the NCUM-G Analysis during ON 2023.

4. Systematic Errors in NCUM-G Forecasts

In this section a brief description about systematic errors in Day-1 (24 hr), Day-3 (72 hr), and Day-5 (120 hr), forecasts during October and November (ON) 2023 are given. The forecast errors with respect to model analysis are presented for Winds, Temperature, and Relative Humidity at 850, 700, 500, and 200 hPa levels (Figures 7-18).

4.1. Winds at 850,700, 500, and 200 hPa levels

Mean winds at 850 hPa level show the presence of low-level north-easterlies over central India, southern peninsular Indian region, and parts of Arabian Sea. The presence of north-easterly winds along the eastern part, especially over Southeast India indicates the effect of NEM during this season. Maximum northeasterly winds are seen along the coastal regions of Somali and South China Seas region. In addition, the presence of strong easterly/ south-easterly winds along the equator is also noted (Figure 7a). Systematic errors in winds from Day-1 forecasts at this level show an easterly wind bias along equator around 80-100^{0}E. A westerly wind bias over the south Arabian Sea around 60^{0}E is seen in Day-1 forecast which is getting enhanced with forecast lead time. Errors in low-level winds enhance around the equatorial regions and this could be due to the enhanced convective activity during the winter season (Figures 7 c-d). Similar systematic errors in winds are also noticed at 700 hPa level. Interestingly Day-1 forecast errors are relatively small compared to the Day-3 and Day-5 forecasts. In addition, westerly wind bias is more prominent at 700 hPa level over the equatorial region and central India in Day-3 and Day-5 forecasts (Figures 8 c-d). In addition, in Day-3 and Day-5 and enhanced cyclonic circulation is also noticed over Head Bay and surrounding coastal regions at both 850 and 700 hPa level.

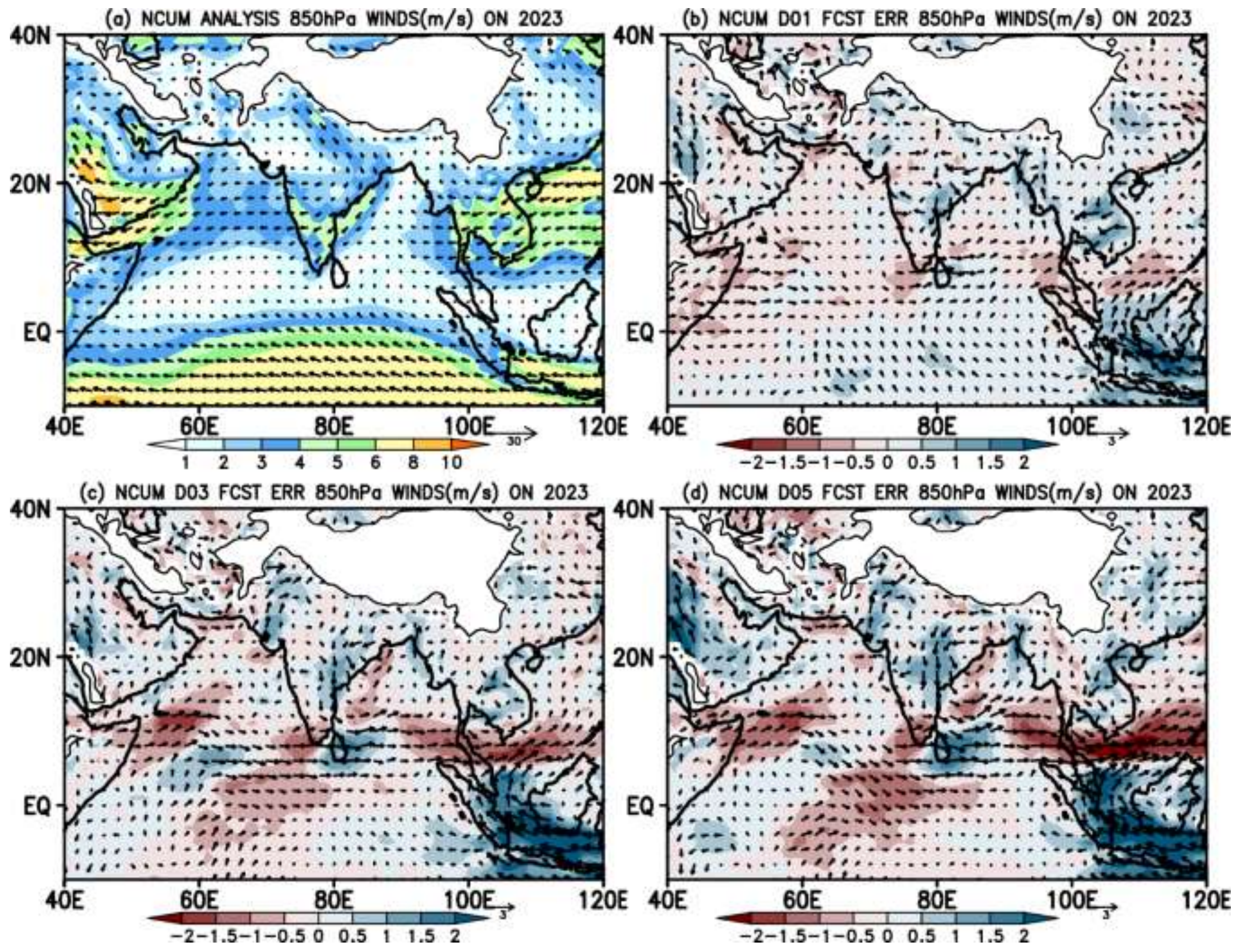

Figure 7. (a) Mean winds and systematic errors (m/s) in (b) Day-1, (c) Day-3, and (d) Day-5 forecasts at 850 hPa during ON 2023.

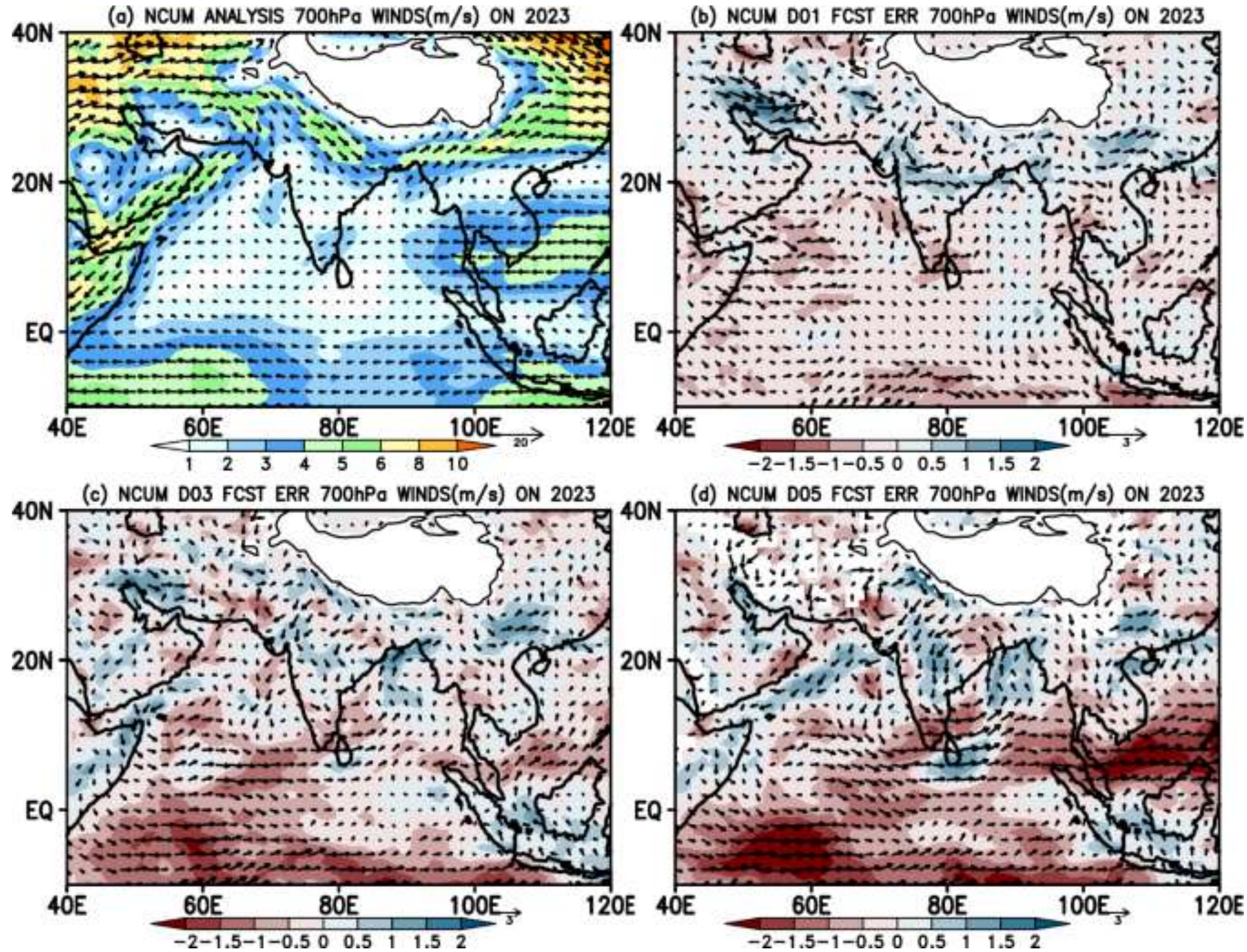

Figure 8. (a) Mean winds and systematic errors (m/s) in (b) Day-1, (c) Day-3, and (d) Day-5 forecasts at 700 hPa during ON 2023.

Mean winds at 500 hPa level show strong westerlies between 30-40^{o}N and these winds penetrated over the central Indian region and turning of winds to north easterlies over AS. In addition, the presence of strong easterlies over BoB is also noted (Figure 9a). Errors in winds at 500 hPa level are relatively small in Day-1 forecasts. The wind bias seen over equatorial regions is enhancing in Day-3 and Day-5 forecasts with westerlies on the west and easterlies on the east indicating active convection around equatorial regions. The enhanced winds exhibit cyclonic circulation over south AS just above the equator in Day-3 and Day-5 forecast around 500 hPa level, which is noteworthy (Figures 9 c-d), and an enhanced anomalous cyclonic circulation covering central India and AS is noted, between the 5-20N latitude belt, in Day-5 forecast. Systematic errors at 200 hPa level winds show enhanced divergent circulation along the equatorial regions on Day-3 and a similar spatial pattern in winds is also seen on Day-5 with enhanced error magnitudes (Figures 10 c-d).

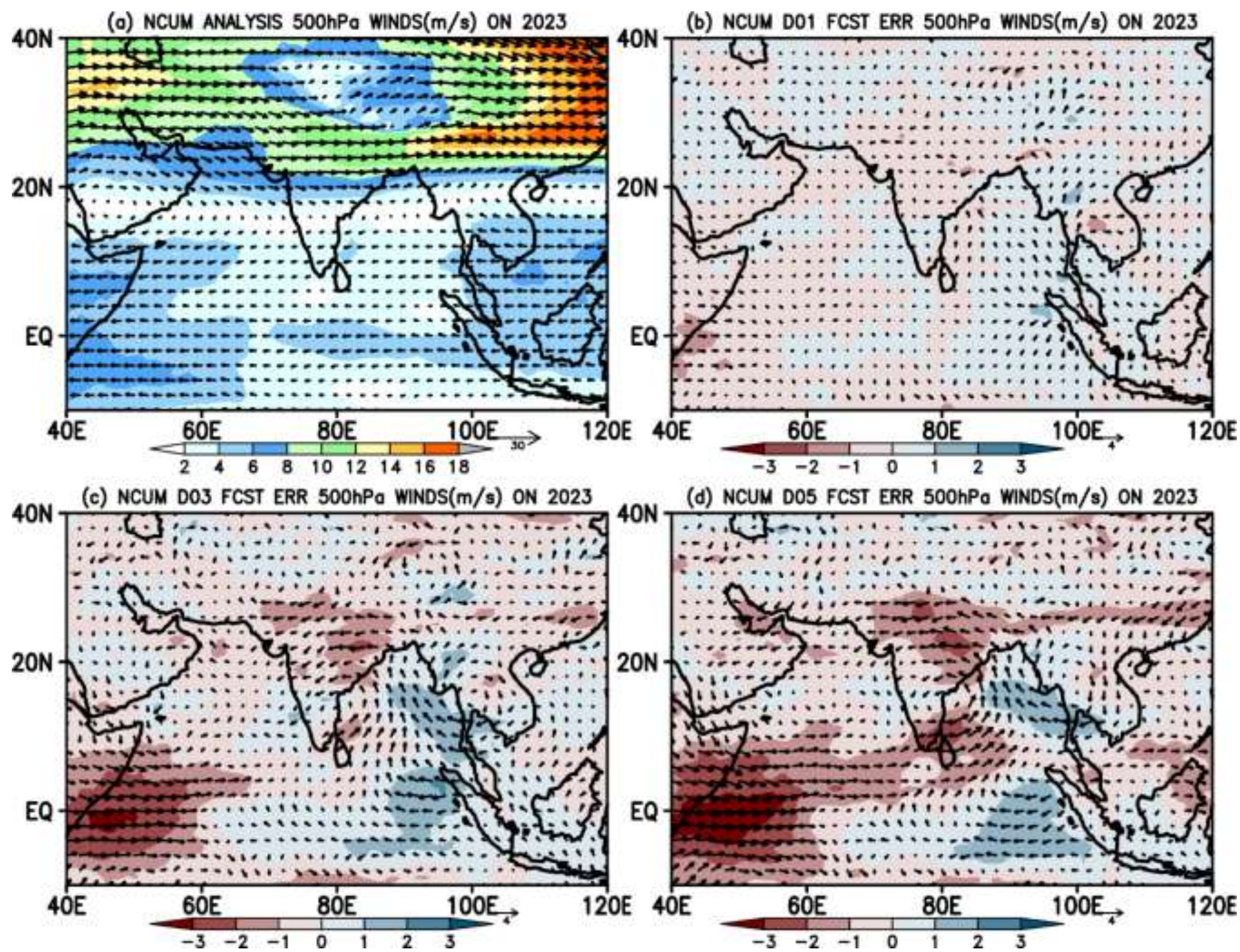

Figure 9. (a) Mean winds and systematic errors (m/s) in (b) Day-1, (c) Day-3, and (d) Day-5 forecasts at 500 hPa during ON 2023.

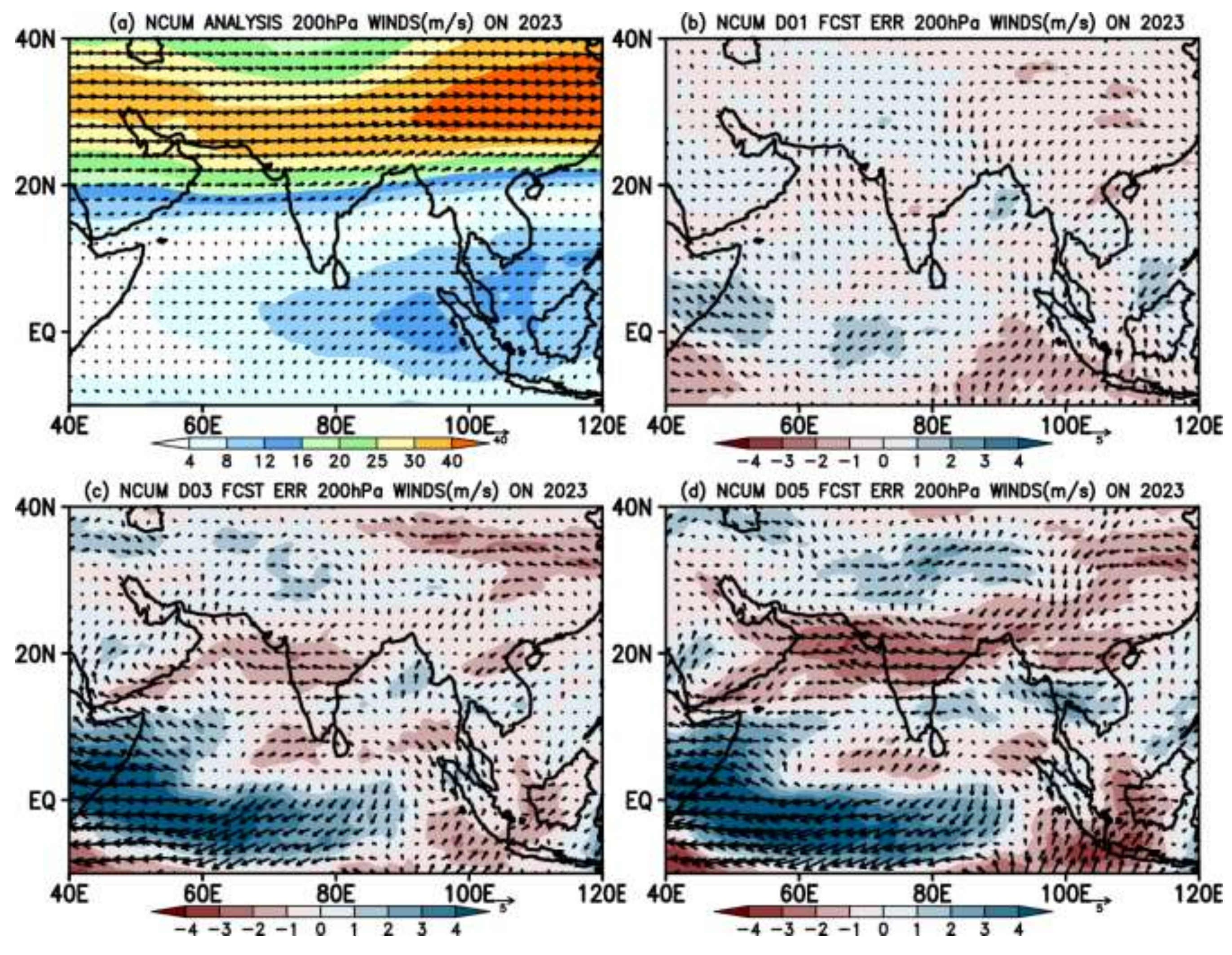

Figure 10. (a) Mean winds and systematic errors (m/s) in (b) Day-1, (c) Day-3, and (d) Day-5 forecasts at 200 hPa during ON 2023.

4.2. Temperature and Relative Humidity

Spatial map of seasonal mean temperature from NCUM-G analysis at 850 hPa shows relatively warm temperatures (18-20^{0}C) over BoB, AS, and surrounding oceanic regions (Figure 11a). The Model shows warm bias (~1^{0}C) occupied over northwestern Indian land mass and over the oceanic regions i.e., AS and BoB, and the magnitude of this bias is increasing over land regions with forecasts lead time (Figure 11 b-d). These error increments at 850 hPa temperatures are also more prominent over eastern African regions. Additionally, the bias over equatorial oceanic regions reverses signs and shows a cold bias, which increases with forecast lead time. On a similar note, the temperature at 700 hPa (Figures 12 b-d) also shows warm bias (~0.5^{0}C) over northwestern Indian land region and cold bias over equatorial oceanic regions. Interesting to see that the bias over AS and BoB reverse sign and now exhibits cold bias compared to the 850hPa level. This cold bias over oceanic regions shows a slight increment with forecast lead time (Figures 12 b-d). At 500 hPa level, temperature exhibits warm bias over most of the Indian land mass and surrounding oceanic regions excluding northwestern Indian region and AS, and the magnitude of the bias is increasing in forecasts with lead time (Figures 13 b-d). However, errors in upper-troposphere (200 hPa) temperatures (Figures 14-b-d) over the Indian land region including most of the Indian Ocean show cold bias. A large patch of warm bias (~0.5^{0}C) over the western equatorial Indian Ocean and over the region between 50-100^{0}E and 30-45^{0}N is prominent in Day-3 and Day-5 forecasts.

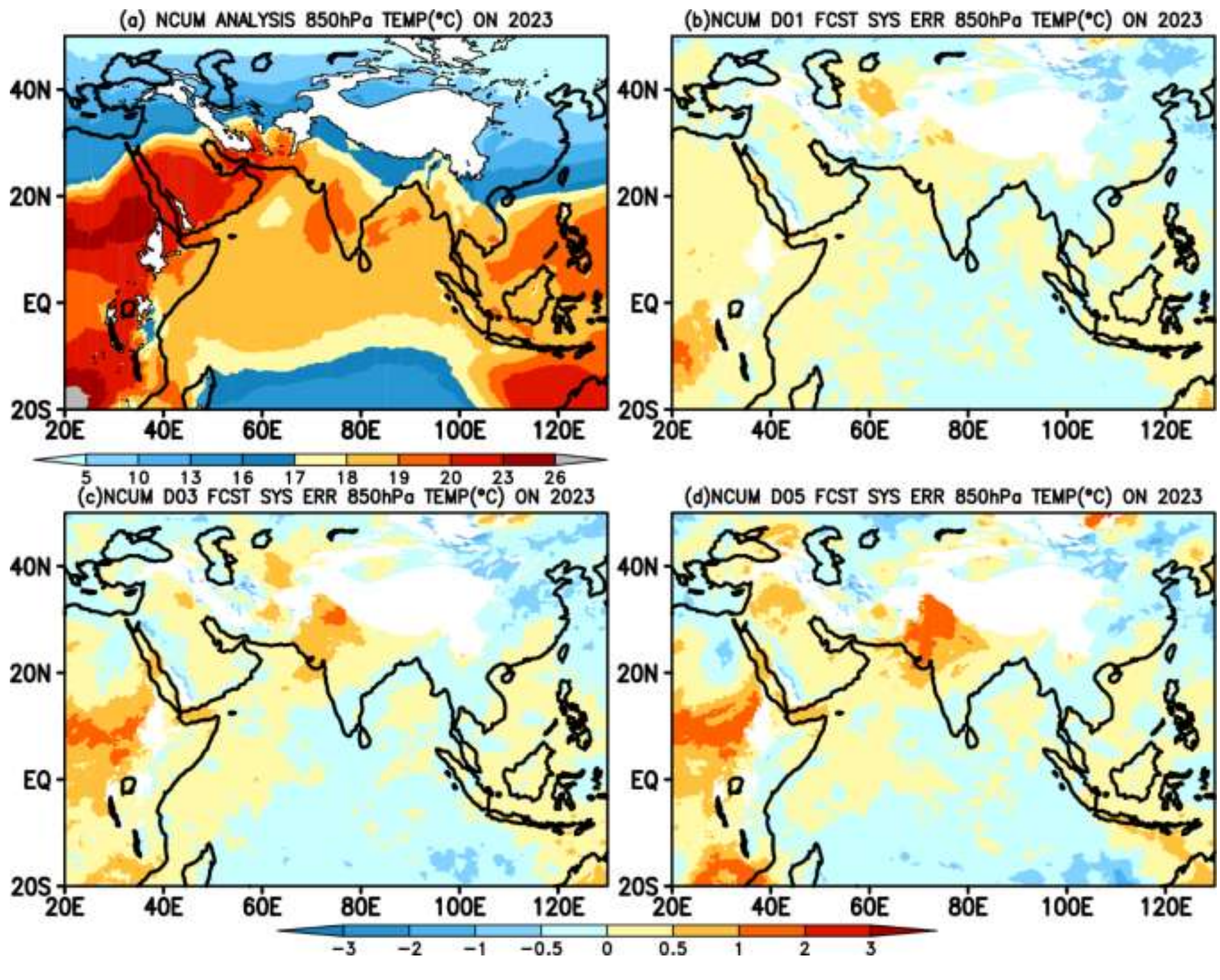

Figure 11. (a) Mean Temperature (Degree Celsius, ^{0}C) and systematic errors (Degree Celsius, ^{0}C) in (b) Day-1, (c) Day-3, and (d) Day-5 forecasts at 850 hPa during ON 2023.

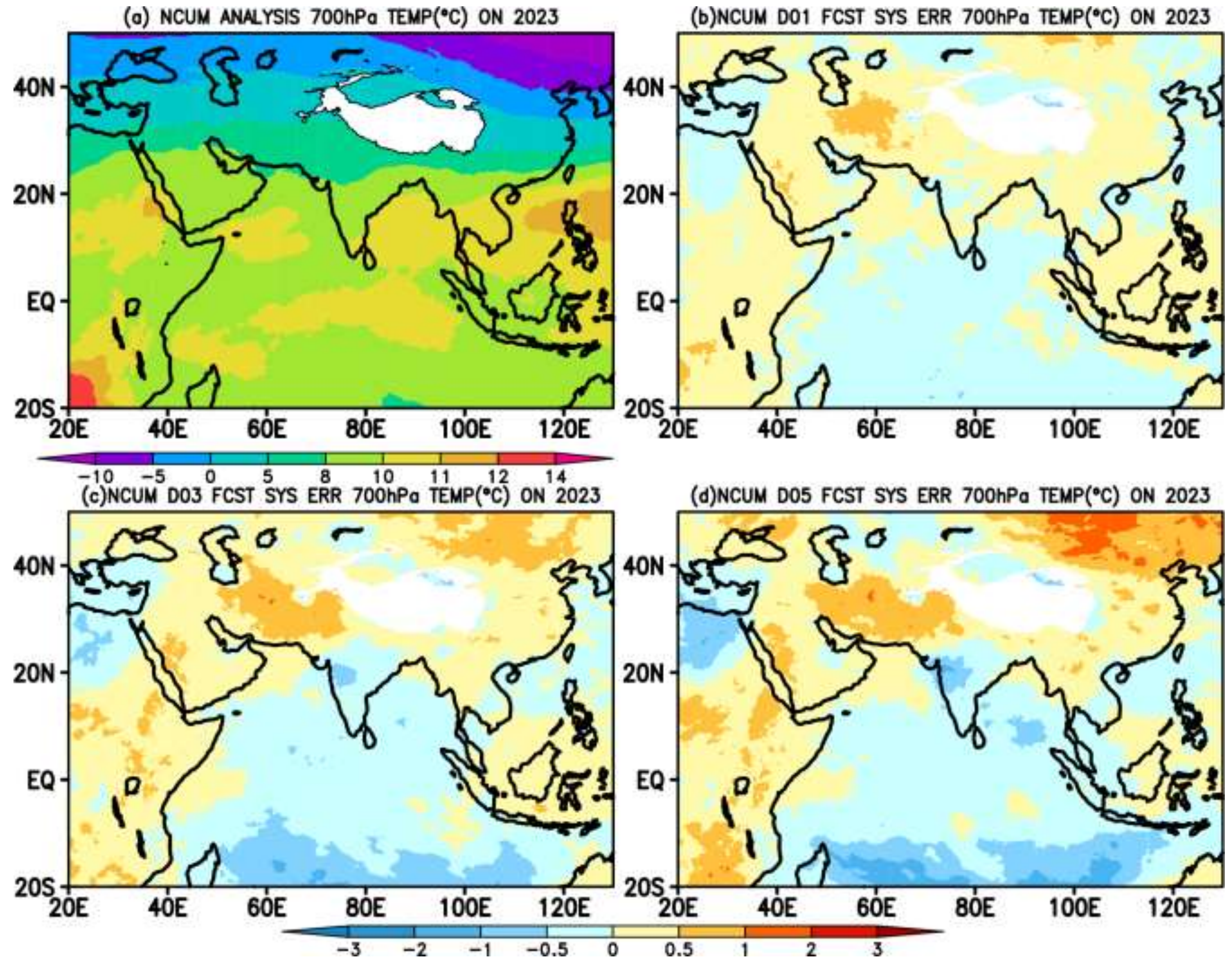

Figure 12. (a) Mean Temperature (Degree Celsius, ^{0}C) and systematic errors (Degree Celsius, ^{0}C) in (b) Day-1, (c) Day-3, and (d) Day-5, forecasts at 700 hPa during ON 2023

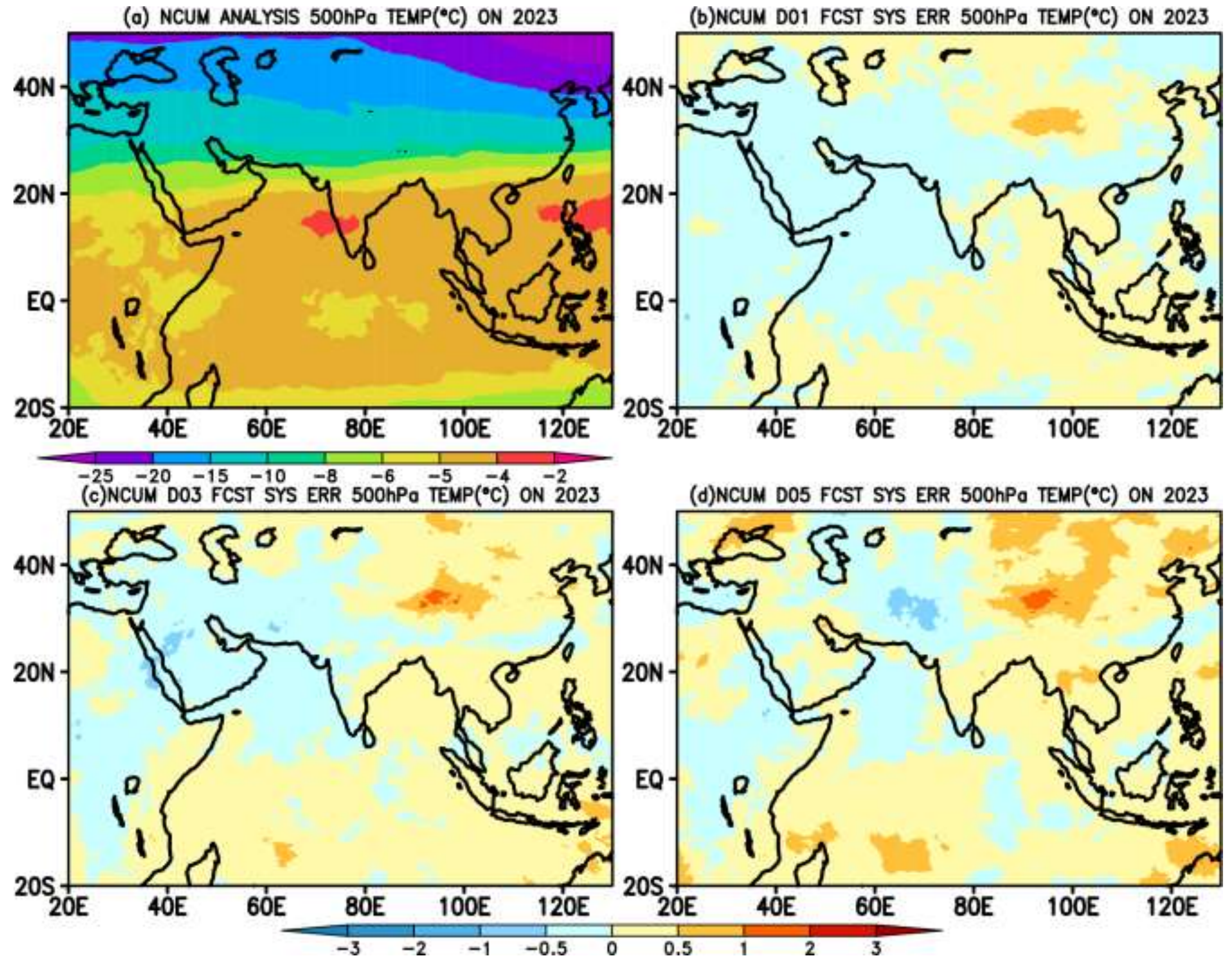

Figure 13. (a) Mean Temperature (Degree Celsius, ^{0}C) and systematic errors (Degree Celsius, ^{0}C) in (b) Day-1, (c) Day-3, and (d) Day-5 forecasts at 500 hPa during ON 2023.

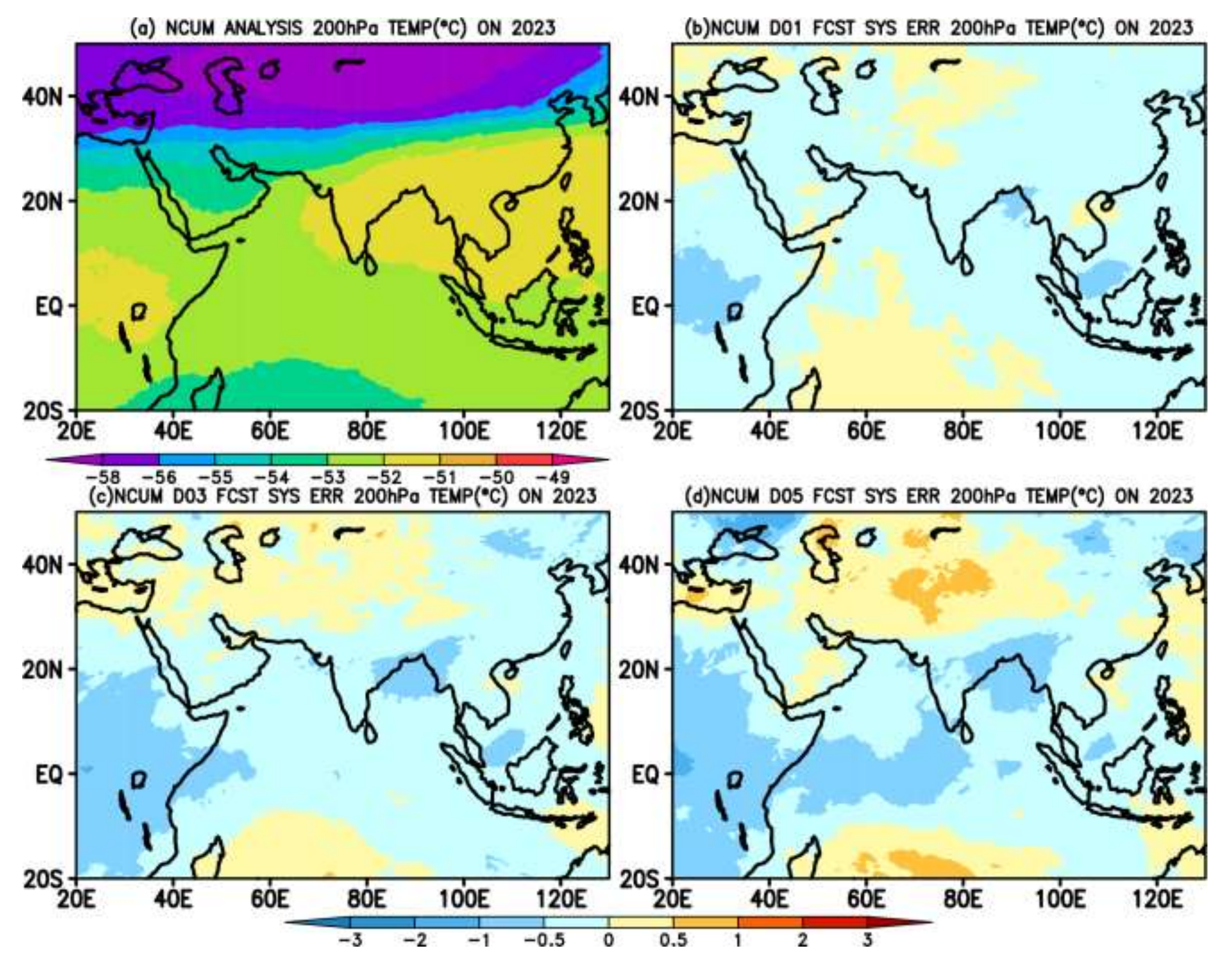

Figure 14. (a) Mean Temperature (Degree Celsius, ^{0}C) and systematic errors (Degree Celsius, ^{0}C) in (b) Day-1, (c) Day-3, and (d) Day-5 forecasts at 200 hPa during ON 2023.

Seasonal mean RH at 850 (Figure 15a) and 700hPa (Figure 16a) levels show large values > 90% over eastern parts of the Indian subcontinent and over some parts of Maritime Continent (MC) regions, and relatively lower RH (dry) values over the northwestern parts of India. Maximum RH values are concentrated over MC consistent with the active convection during the winter period. Systematic errors at 850hPa level show dry bias over the Indian land region, most of the Indian subcontinent, and regions surrounding MC; and this dryness is enhancing with forecasts lead time (Figures 15 c-d), which could possibly influence the MJO propagation through MC in NCUM-G. Interestingly the dry bias observed over the Indian land region excluding peninsular India region at 850hPa level changed sign to positive and moist bias is seen at 700hPa level (Figures 16 b-d). However, the dryness over MC and surrounding regions persists at all the levels from

700 to 200hPa (Figures 16, 17, and 18). In contrast, the moist bias south of the equator is getting intensified in the Day-3 and Day-5 forecast, and the entire column is occupied with excess moisture from 700 to 500hPa levels (Figures 16 and 17). At 200hPa, RH exhibits dry bias over the northwestern Indian region, peninsular region, northern AS, and the south of the equator. Notably, these dry biases become more pronounced with an increase in forecast lead time, as illustrated in Figures 18 c-d.

In the next section, a brief description of systematic errors in the model forecasts is presented for key surface variables such as 2m Temperature (Figure 19), 10m winds (Figure 20), and Total Precipitable water (PWAT; Figure 21). The errors are computed against the NCUM-G analysis.

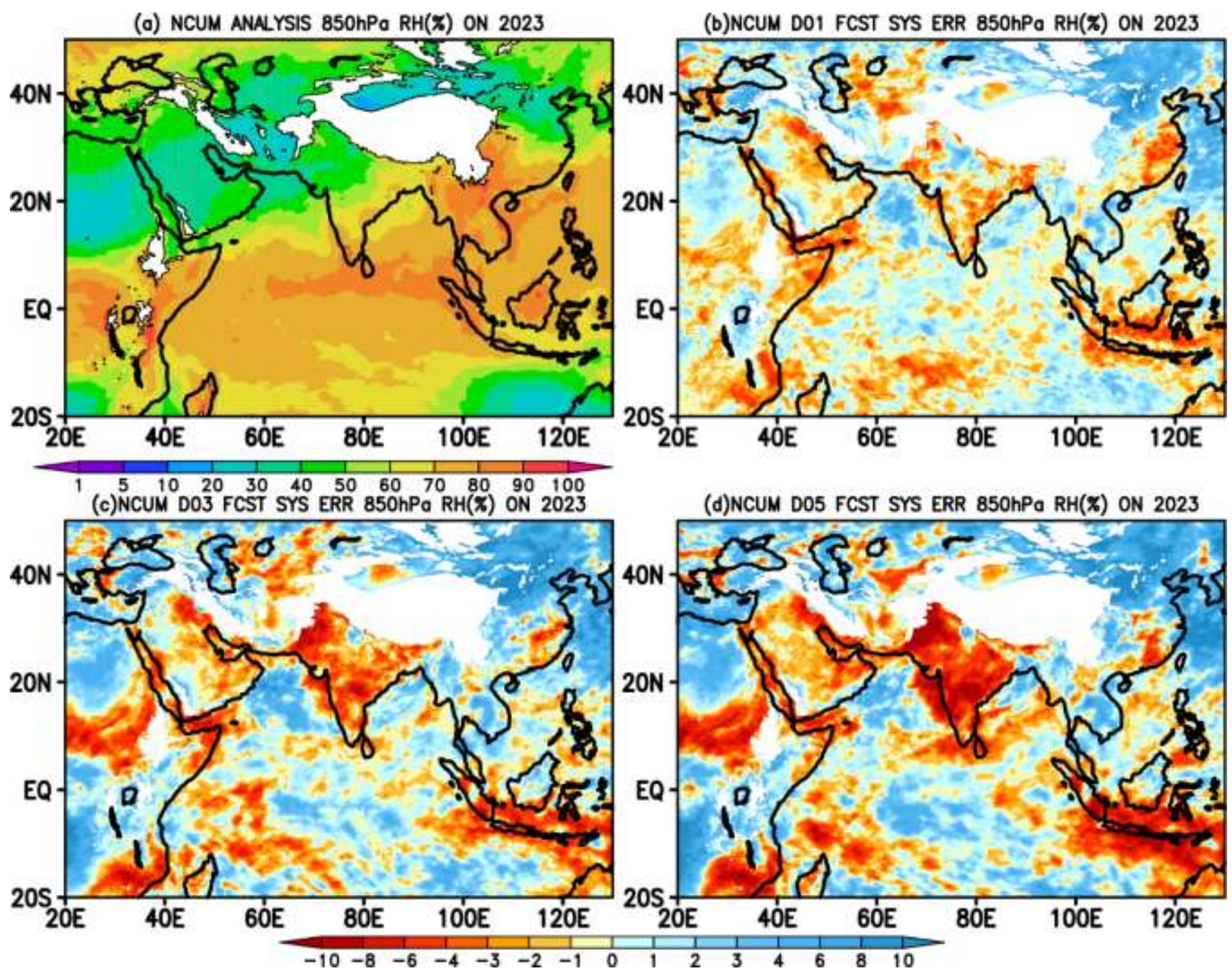

Figure 15. (a) Mean Relative Humidity (%) and systematic errors (%) in (b) Day-1, (c) Day-3, and (d) Day-5 forecasts at 850 hPa during ON 2023.

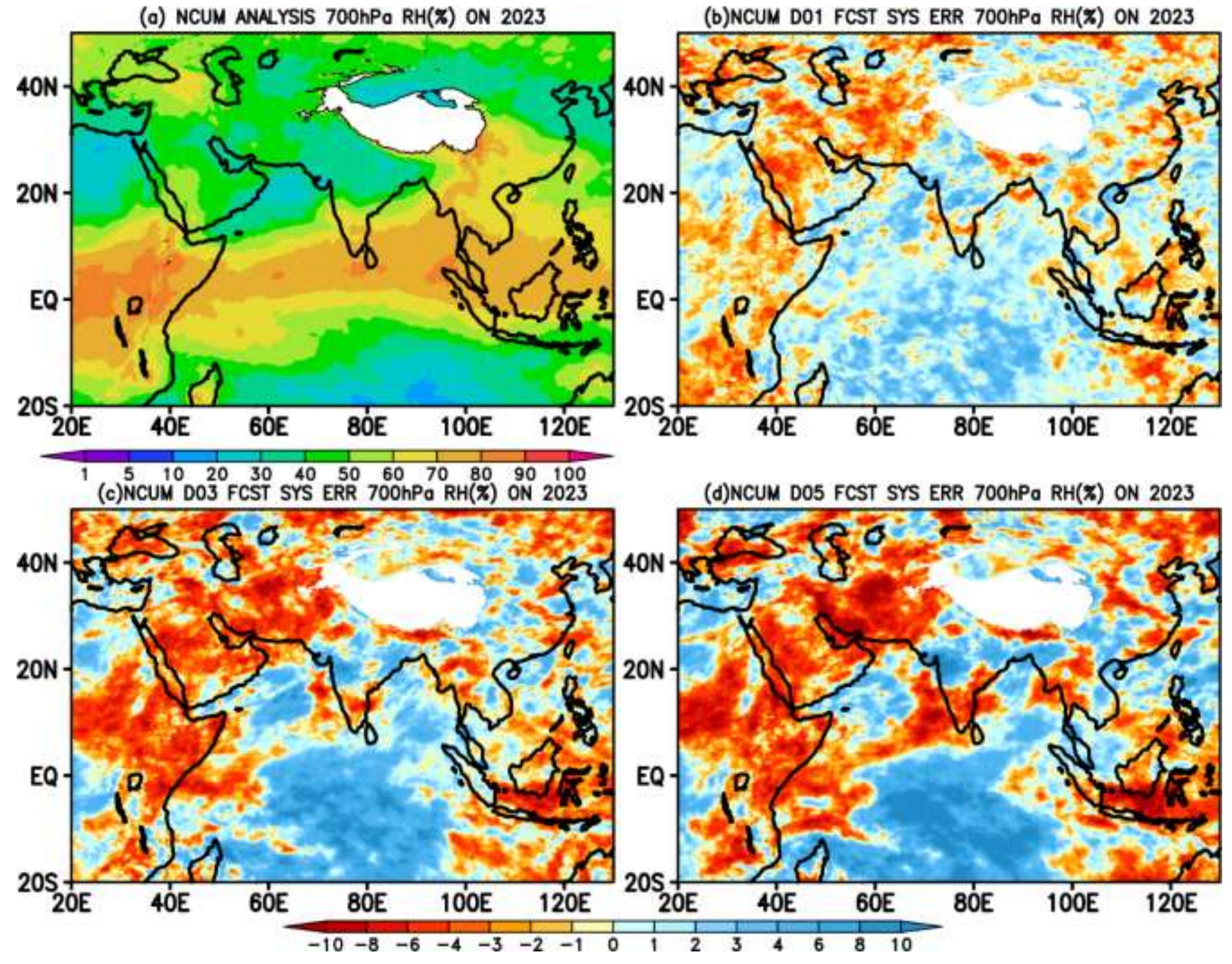

Figure 16. (a) Mean Relative Humidity (%) and systematic errors (%) in (b) Day-1, (c) Day-3, and (d) Day-5 forecasts at 700 hPa during ON 2023.

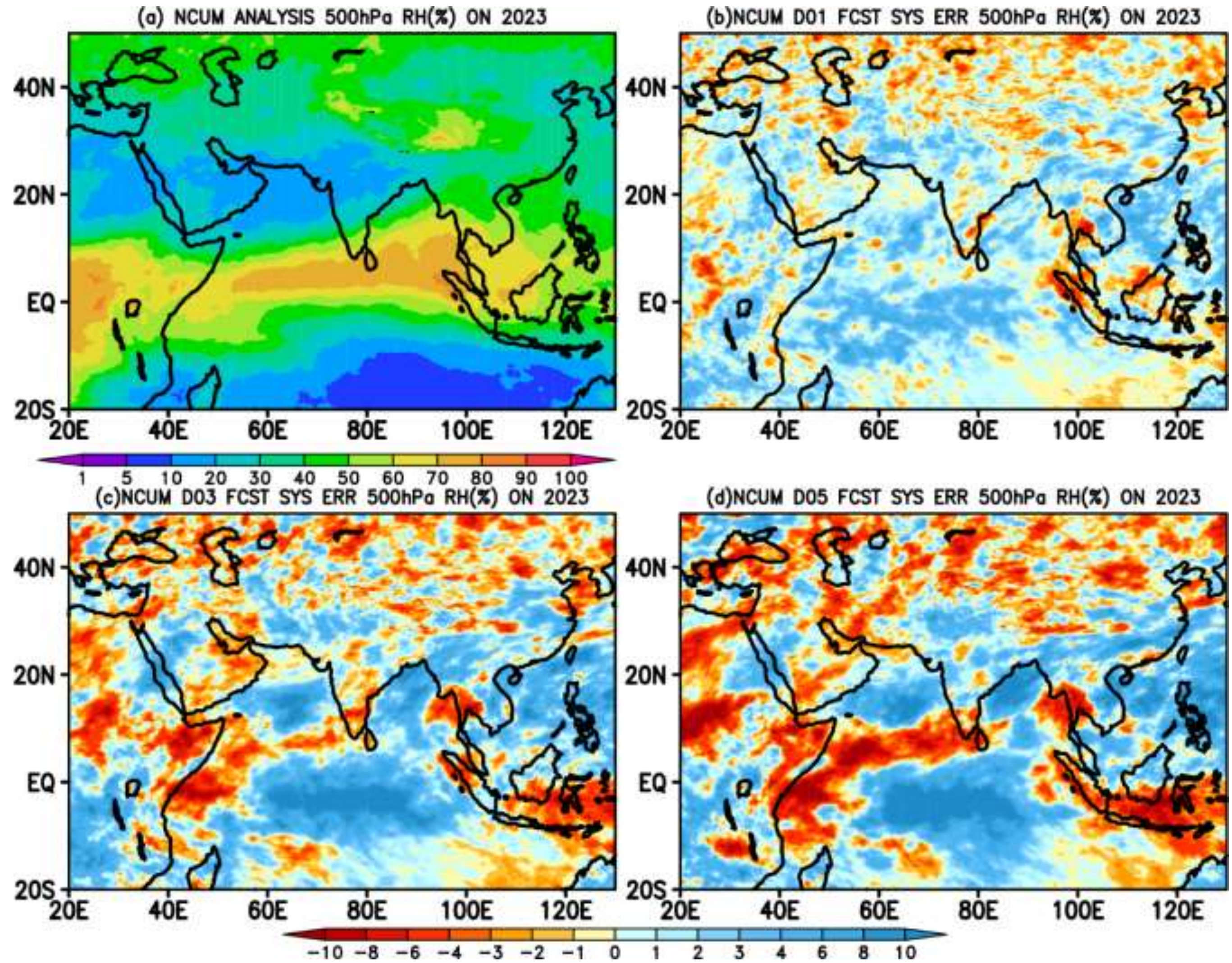

Figure 17. (a) Mean Relative Humidity (%) and systematic errors (%) in (b) Day-1, (c) Day-3, and (d) Day-5 forecasts at 500 hPa during ON 2023.

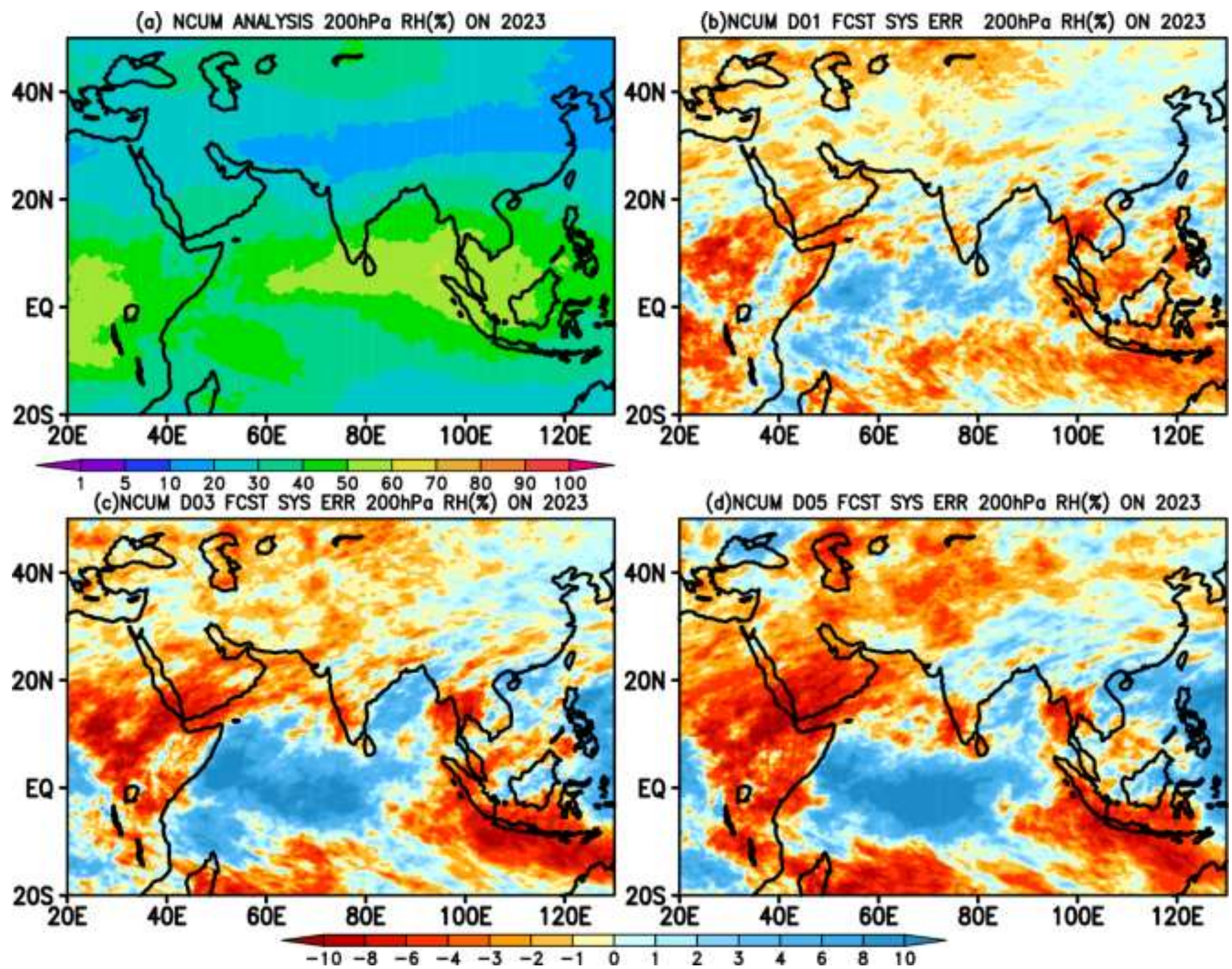

Figure 18. (a) Mean Relative Humidity (%) and systematic errors (%) in (b) Day-1, (c) Day-3, and (d) Da y-5 forecasts at 200 hPa during ON 2023.

4.3. Surface (10m) winds

The seasonal mean winds at 10m from the analysis (Figure 19a) reveal the prevalence of strong Northeasterlies over the Bay of Bengal (BoB) and Arabian Sea (AS), reaching their peak intensity around the open AS, African coast, and South China Sea. Moreover, easterlies are also observed in the analysis beyond the equator. The systematic errors in the forecasts (Figures 19 b-d) depict few notable features; 1) Presence of feeble cyclonic circulation over BoB is noticed in Day-1 (Figure 19b). 2) Presence of south-westerlies over AS and BoB in Day-3 and Day-5 (Figures 19c and d).

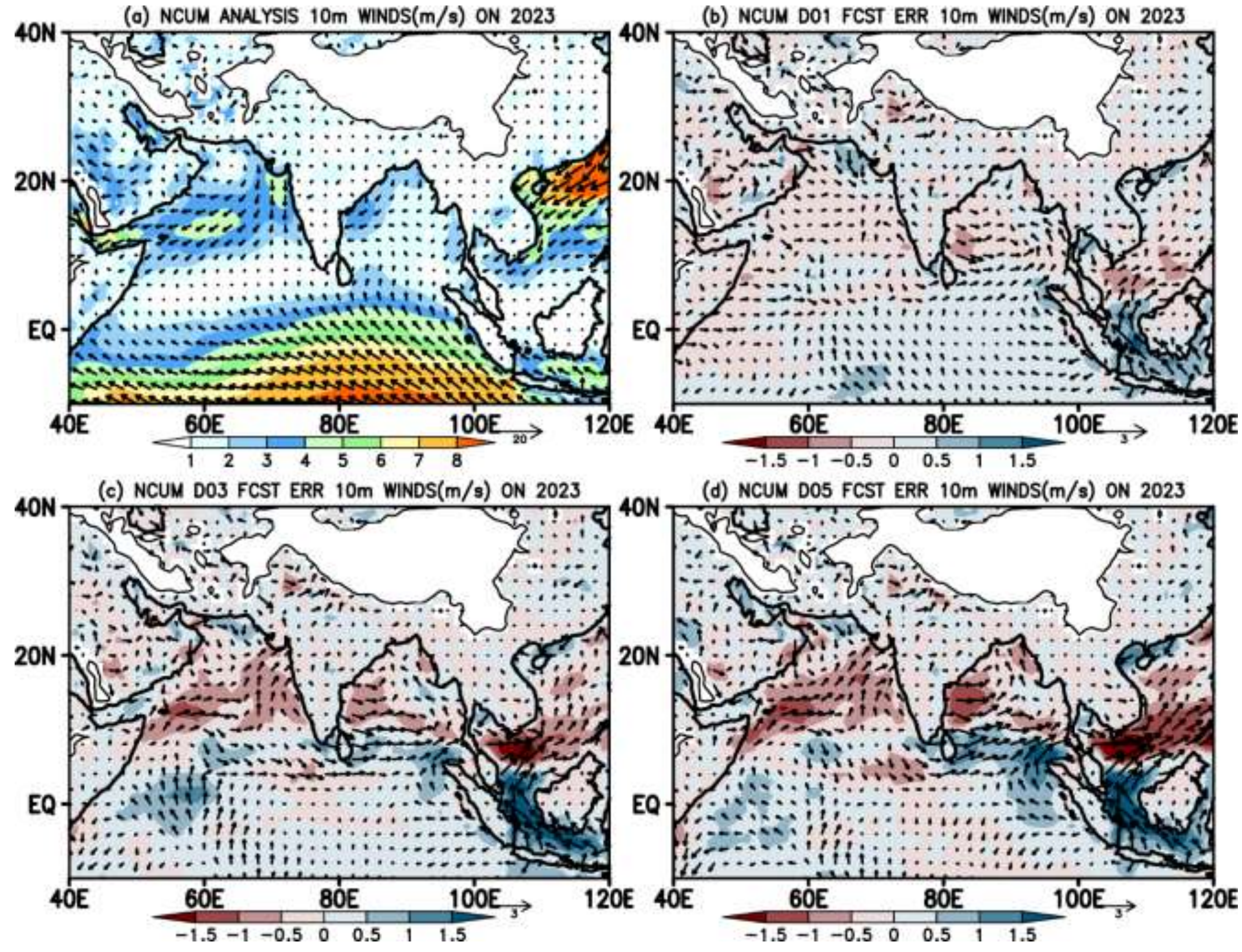

Figure 19. (a) Mean winds at 10m height and systematic errors (m/s) in (b) Day-1, (c) Day-3, and (d) Day-5 forecasts during ON 2023.

4.4. Temperature at 2m

Seasonal mean temperature ranges between 24-30^{0}C all over the Indian land and surrounding oceanic regions (Figure 20a). Systematic errors (Figures 20b-d) show a relatively cold bias (< -1^{0}C) over Indian land regions except northwestern region and these cold biases are increasing with forecast lead time. This can be attributed to the presence of arid regions and resulting in large sensible heat flux and dry north-westerly winds from the northwest towards Indian region (Figure 19). In addition, most of the BoB and parts of MC and surrounding regions exhibited warm bias in the range of 0-0.5^{0}C in all the forecast lead times. In addition, model temperature errors also exhibit a cold bias over the AS. It is noted that the magnitude of temperature bias is consistent in all the lead times stated here (Figures 20b-d).

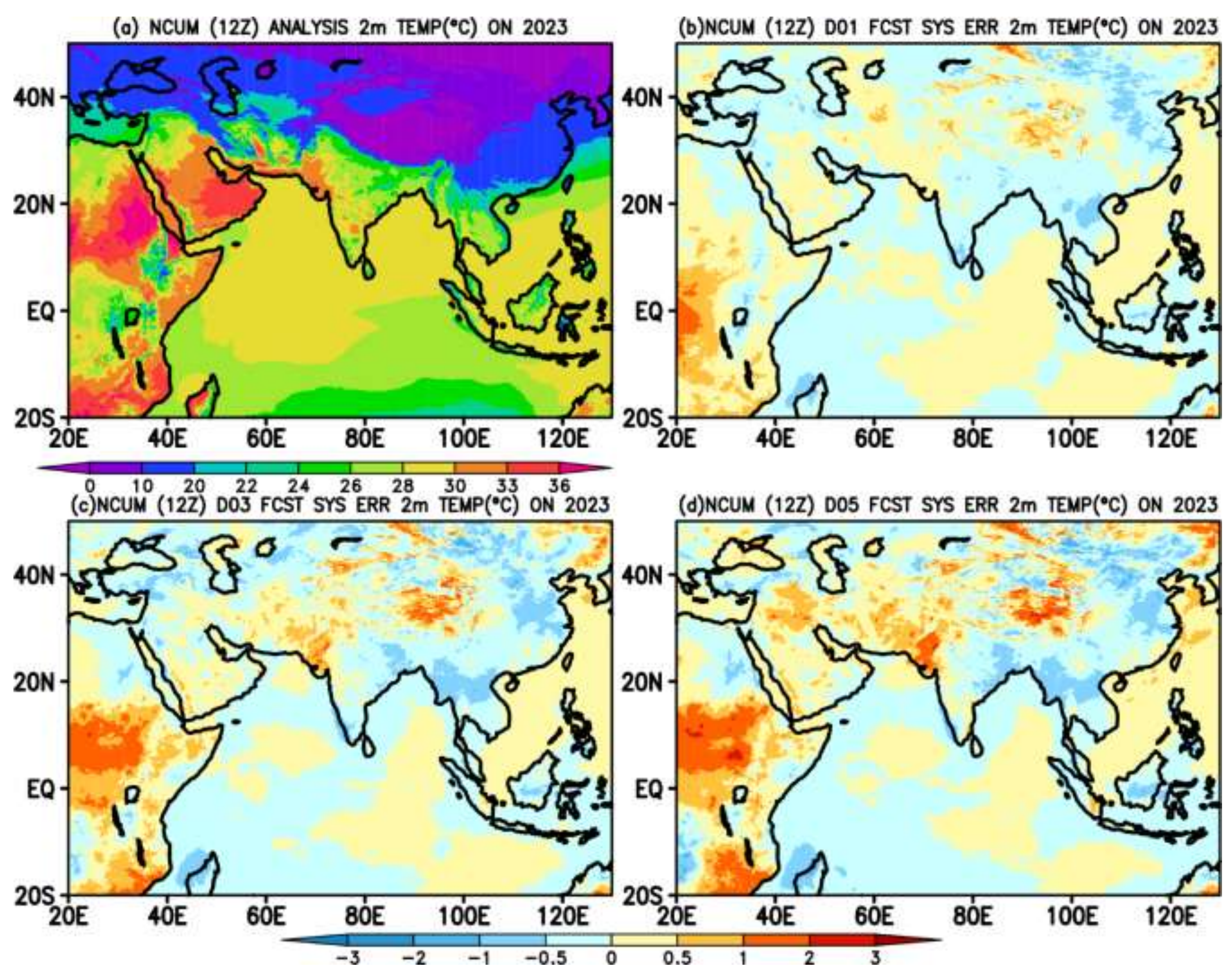

Figure 20. (a) Mean Temperature at 2m height and systematic errors (Degree Celsius, ^{0}C) in (b) Day-1, (c) Day-3, and (d) Day-5 forecasts during ON 2023.

4.5. Total Precipitable Water (PWAT)

Seasonal mean PWAT shows a large value (> 55 mm) around the equatorial regions (Figure 21a), especially over some parts of MC owing to the presence of winter-time convection and its eastward movement (MJO) active conditions over these regions. In contrast, most of the northern and central Indian regions are dry with very low PWAT values (5-15 mm, Figure 21a). Systematic error in PWAT (Figures 21 b-d) shows a column dryness over Indian land regions on Day-1, this dryness in column is enhancing with forecast lead time and its magnitude is maximum in Day-5 (Figures 21 c-d). Large positive (negative) PWAT biases are seen over the AS (MC) regions. This excess (deficit) column water over the equatorial regions could possibly influences the MJO convection and propagation towards the west Pacific.

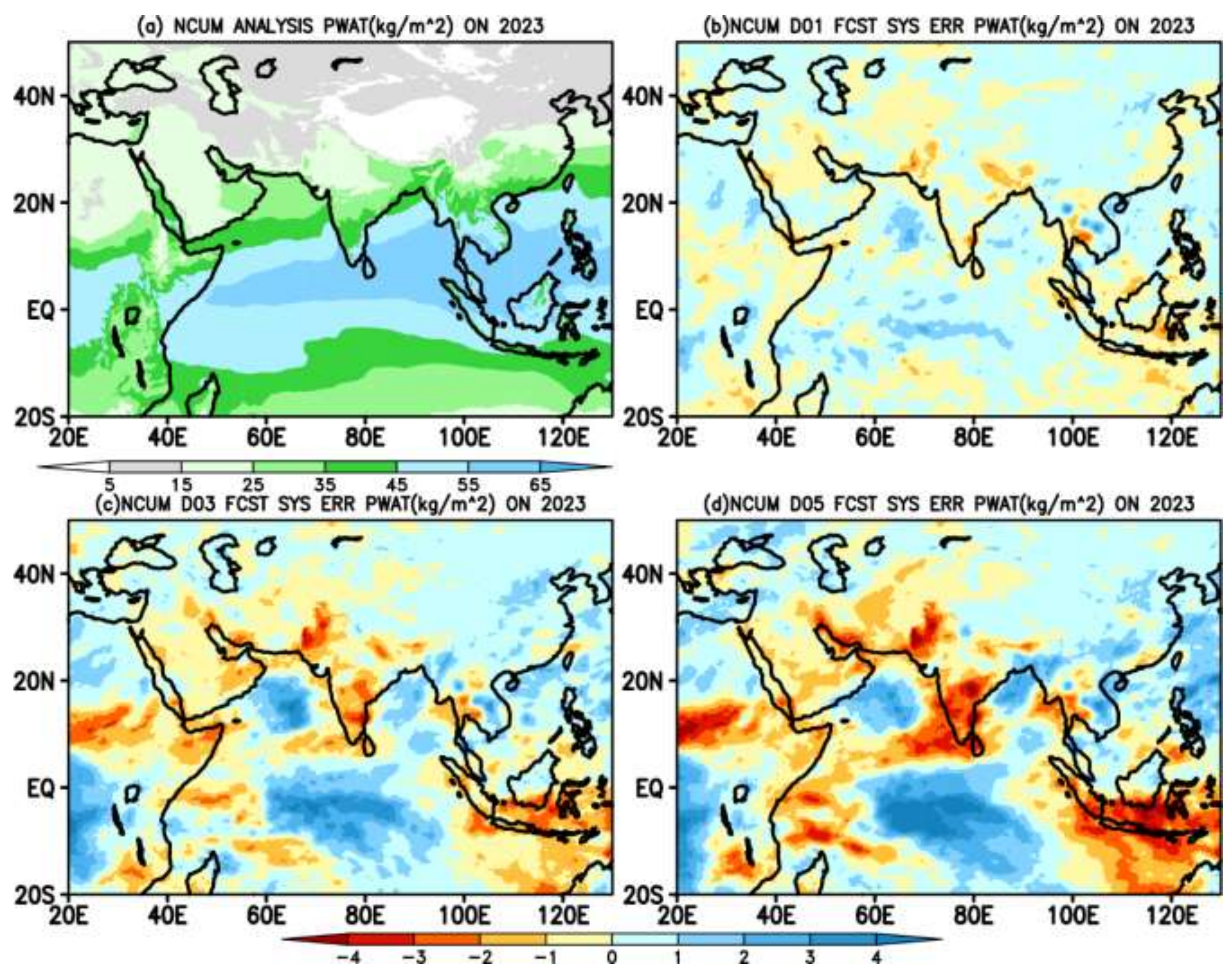

Figure 21. (a) Mean total precipitable water (PWAT) up to model levels and systematic errors (mm) in (b) Day-1, (c) Day-3, and (d) Day-5 forecasts during ON 2023.

5. Rainfall Forecast Verification during ON 2023

In general, during ON, rainfall primarily occurs over the meteorological sub-divisions of Tamil Nadu, coastal Andhra Pradesh, and parts of Kerala. Nearly 45% of the annual rainfall occurs during this season over these subdivisions. Further, this season is usually considered as cyclone season over the North Indian Ocean (NIO) where the systems move west/northwest wards affecting the coastal regions of southeast peninsular India. In addition, *Easterly waves* that moves across peninsular India also contribute significantly to the ON rainfall activity. Another important feature is the establishment of a trough in the southern BoB and associated with that we usually see cyclonic circulations. This LP area draws tropical disturbances such as cyclones and easterly waves causing widespread rainfall over Tamil Nadu and neighboring subdivisions. During ON 2023, four low-pressure systems formed over BoB that have influenced the rainfall activity over south peninsular India.

In this section, verification of NCUM-G model rainfall forecasts is presented for ON 2023. The daily accumulated rainfall forecasts are verified against the NCMRWF-IMD merged Satellite and gauge rainfall product. The discussion presented in this section is confined to mean and mean error (ME) over the India region. Further, this section also quantifies forecast skill using standard verification metrics, namely, the probability of detection (POD), false alarm ratio (FAR), and critical success index (CSI) which are described in standard textbooks (Wilks, 2011, Jolliffe and Stephenson, 2012); and Symmetric extremal dependence index (SEDI), a metric for extreme and rare events (Stephenson et al 2008, Ashrit et al 2015b, Sharma et al 2021). Furthermore, the Total Interest is also computed, which represents a measure computed through fuzzy logic for each forecast/observation object pair based on user-defined weights.

5.1. Mean and Mean Error

The observed and forecast mean rainfall during ON 2023 is shown in Figure 22. Observations indicate the highest mean rainfall exceeding 15mm/day is seen over the southern parts of peninsular India, south BoB, and equatorial oceanic regions. Moderate rainfall (2-4 mm/day) is seen over the Jammu and Kashmir regions where the effect of western disturbances is more prominent which brings a significant amount of rain over these regions. The panels in the middle row, Figures 22 b-d show the Day-1, Day-3, and Day-5 NCUM-G forecast rainfall averaged during the ON2023 period. The observed peak in rainfall amounts is well predicted in all the forecast lead times. However, it is found that the NCUM-G forecast overestimates mean rainfall amounts and spatial distribution over the north-eastern regions, BOB, and the oceanic regions around the equator. Apart from this most of the Indian subcontinent is dry with no convection in both observations and forecasts (Figures 22 a-d). Now, to further quantification forecast mean errors (ME) are computed against the observation. The panels in the bottom row show rainfall ME (Figures 22 e-g) in predicted rainfall indicating wet bias (blue) over southern parts of the oceanic regions consistent with the mean rainfall patterns (Figures 22 b-d). Small dry bias regions are noticed over Sri Lanka, Bangladesh, and some parts of Tamil Nadu in the rainfall forecasts and the magnitude of dry bias is increases with lead time (Figures 22 e-g).

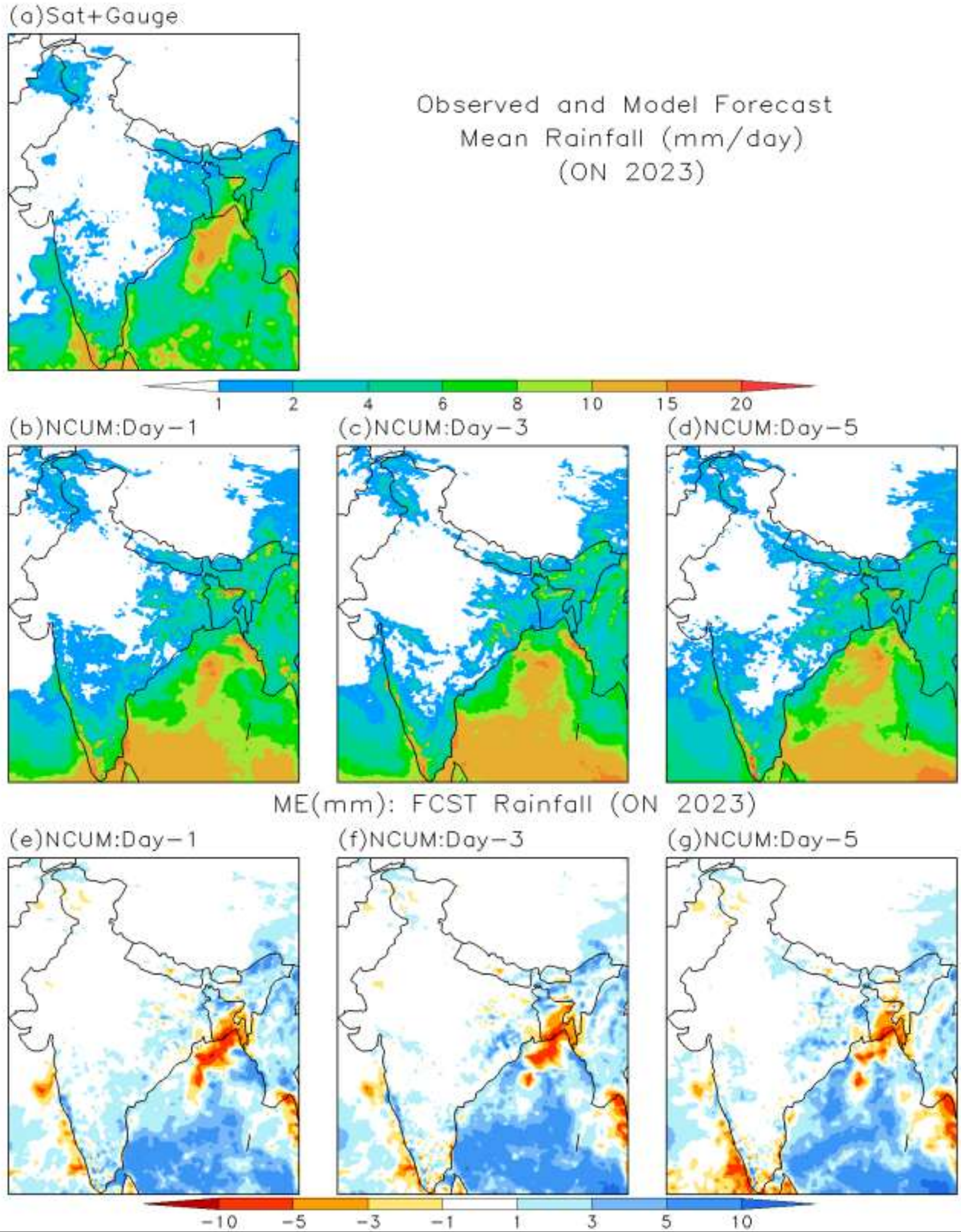

Figure 22. Accumulated ON rainfall (mm) in (a) Observations and (b) Day-1, (c) Day-3, and (d) Day-5 forecasts. Bottom panels (e), (f), and (g) show Mean Error (ME) in Day-1, Day-3, and Day-5 forecasts, respectively.

5.2. Categorical Scores of Rainfall Forecasts

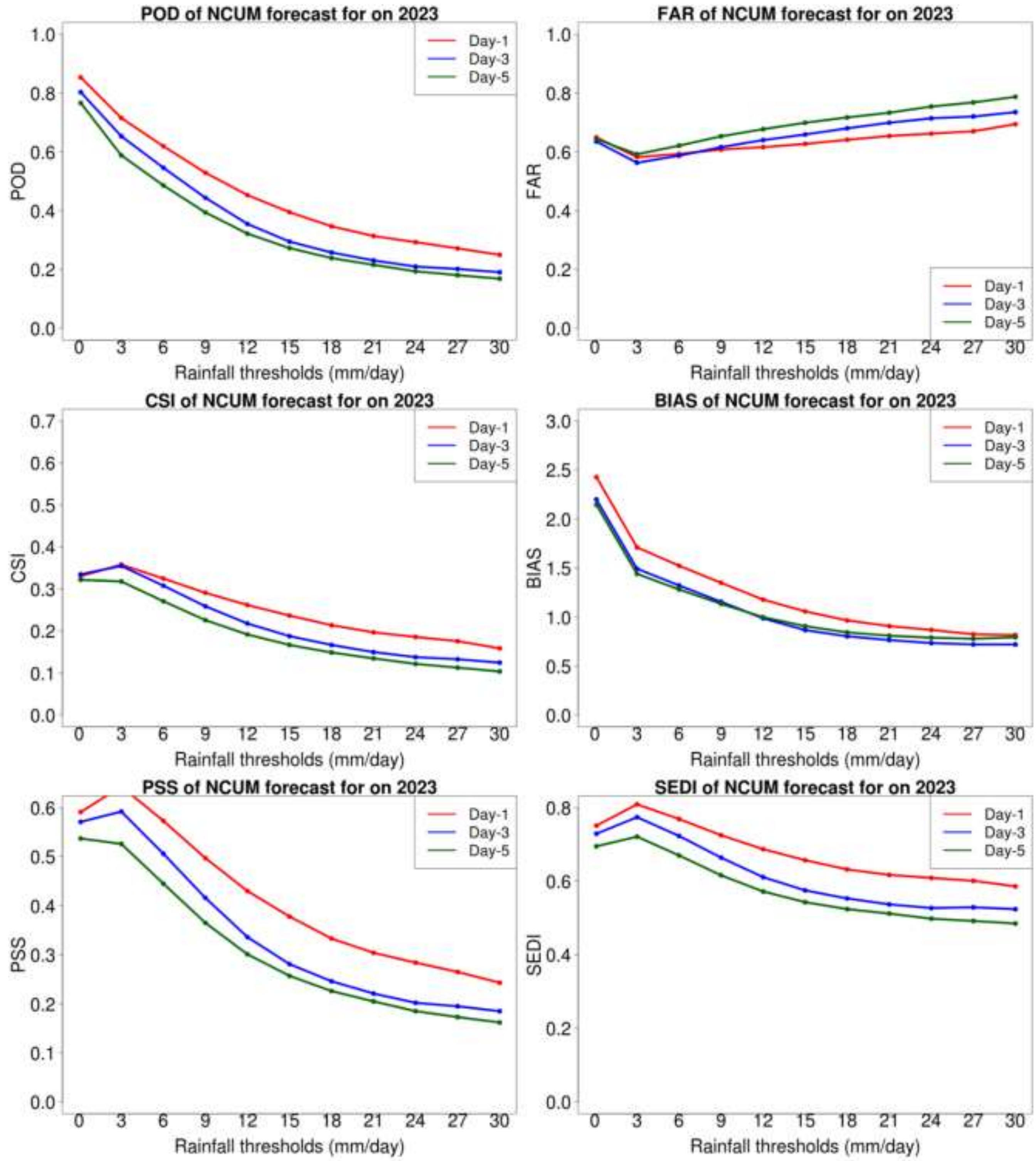

Figure 23. Categorical all India Rainfall scores POD (*top left*), FAR (*top right*), CSI (*middle left*), BIAS (*middle right*), PSS (*bottom left*), and SEDI (*bottom right*).

To further quantifying the model rainfall forecasts, categorical skill scores are computed over the Indian subcontinent (Figure 23). The categorical approach of verifying quantitative precipitation forecast (QPF) is generally based on the 2 x 2 contingency table which is evaluated for each threshold. Verification scores are presented for rainfall of up to 30mm/day. For different rainfall thresholds, POD and FAR show decrease and increase in scores, respectively. The BIAS score (frequency bias) indicates that forecasts overestimate the frequency up to 9mm/day thresholds. The values of the Peirce's skill score (PSS) and SEDI, all are high for rainfall up to 3-9 mm/day suggesting reasonable skill. PSS score shows a very sharp decrease as the threshold varies. Overall, the skill is not bias-free. For higher rainfall thresholds (> 10 mm/day), frequency bias is almost constant, but the skill is low as indicated by CSI, PSS, and SEDI (Figure 23).

5.3. Total Interest

Total Interest is a measure of which is computed by fuzzy logic for each forecast/observation object pair based on user-defined weights. It involves defining objects in the forecast and observation fields, computing attributes for each of those objects, and then calculating differences between their attributes. The computed interest values are used to match objects across fields and merge objects within the same field. The performance of global models can be evaluated based on their ability to accurately forecast certain phenomena. This involves comparing the model's forecasts to actual observations. When the model's forecasts align closely with the observations, the model is considered to have performed well.

For the Indian domain's rainfall in October and November 2023, the Total Interest values from MODE represent the alignment degree between the forecasts of four global models and the actual observed rainfall. A higher Total Interest value suggests a better model performance as it indicates a closer match between the forecast and observed data. The Figure 24 illustrates the Total Interest from MODE for convolution threshold (CT) 20.0 mm/day rainfall predictions over five days, as forecasted by four global models: NCUM, United Kingdom Meteorological Office Global Model (UKMO), Global Forecast System (GFS), and National Centers for Environmental Prediction's (NCEP). Each day is represented by a separate bar graph, with each model's predictions illustrated in different colored bars. The Total Interest values range between approximately 0.75 and 0.95. This data suggests a consistency in the performance of each global model across the five days. All models maintain a relatively stable Total Interest value throughout this period, indicating reliability in their predictive capabilities for rainfall over the Indian domain.

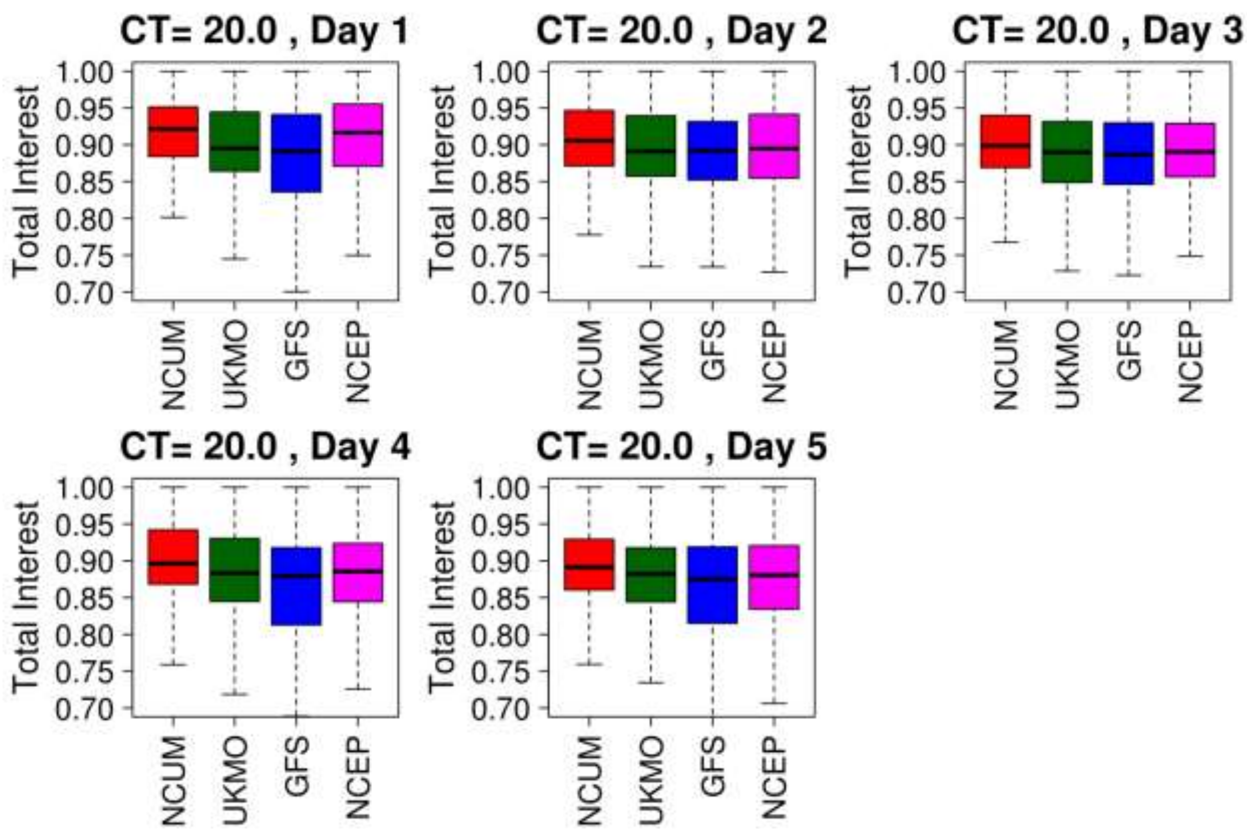

Figure 24. Total Interest from MODE for convolution threshold (CT) 20.0 mm/day rainfall predictions over five days, as forecasted by four global models: NCUM, UKMO, GFS, and NCEP.

6. Significant Weather Events during Oct-Nov 2023

This section provides a brief summary report on the verification of the NCMRWF model forecasts for the two systems: the Extremely Severe Cyclonic Storm (ESCS) “Tej” over the Arabian Sea during 20-24 Oct 2023 and Very Severe Cyclonic Storm (VSCS) “Hamoon” over Bay of Bengal during 21-25 Oct 2023. Verification of the forecast tracks and intensity is presented for NCMRWF Unified Models; NCUM-G (12km grid resolution), NCMRWF Global Ensemble Prediction System (NEPS-G; 12km grid resolution), NCMRWF Regional Unified Model (NCUM-R; 4km grid resolution) for both 00UTC and 12UTC runs; and NCMRWF Regional Ensemble Prediction System (NEPS-R; 4km grid resolution) for 00UTC runs. Forecast verification is presented for model-predicted tracks and intensity against the IMD best track data.

6.1. Arabian Sea ESCS 'Tej' during 20-24 Oct 2023

This subsection briefly summarizes on the verification of the NCMRWF model forecasts for the recent ESCS ‘Tej’ during 20-24 Oct 2023, which developed over the Arabian Sea (AS). ‘Tej’ crossed the Yemen coast close to South of Al Ghaidah in the early hours (between 02:30 and 03:30 hours IST) of 24th Oct as a VSCS with intensity of 65 knots gusting to 75 knots (120-130 kmph gusting to 140 kmph). Verification of the forecasts is presented for all NCMRWF Unified Models; NCUM-G (12km grid resolution) and NEPS-G mean (12km grid resolution) for both 00UTC and 12UTC runs.

6.1.1. Forecast Tracks and Strike Probability

The observed and predicted tracks based on 00UTC of 23rd Oct 2023 are shown in Figure 25 (top). *All the predicted tracks indicated that ESCS ‘Tej’ would track towards Yemen.* The strike probability (Figure 25; bottom) based on the 23 (1 control+22 perturbed) member NEPS-G ensemble indicate that the cyclone would approach the Yemen coast in forecast based on 23rd May 2023.

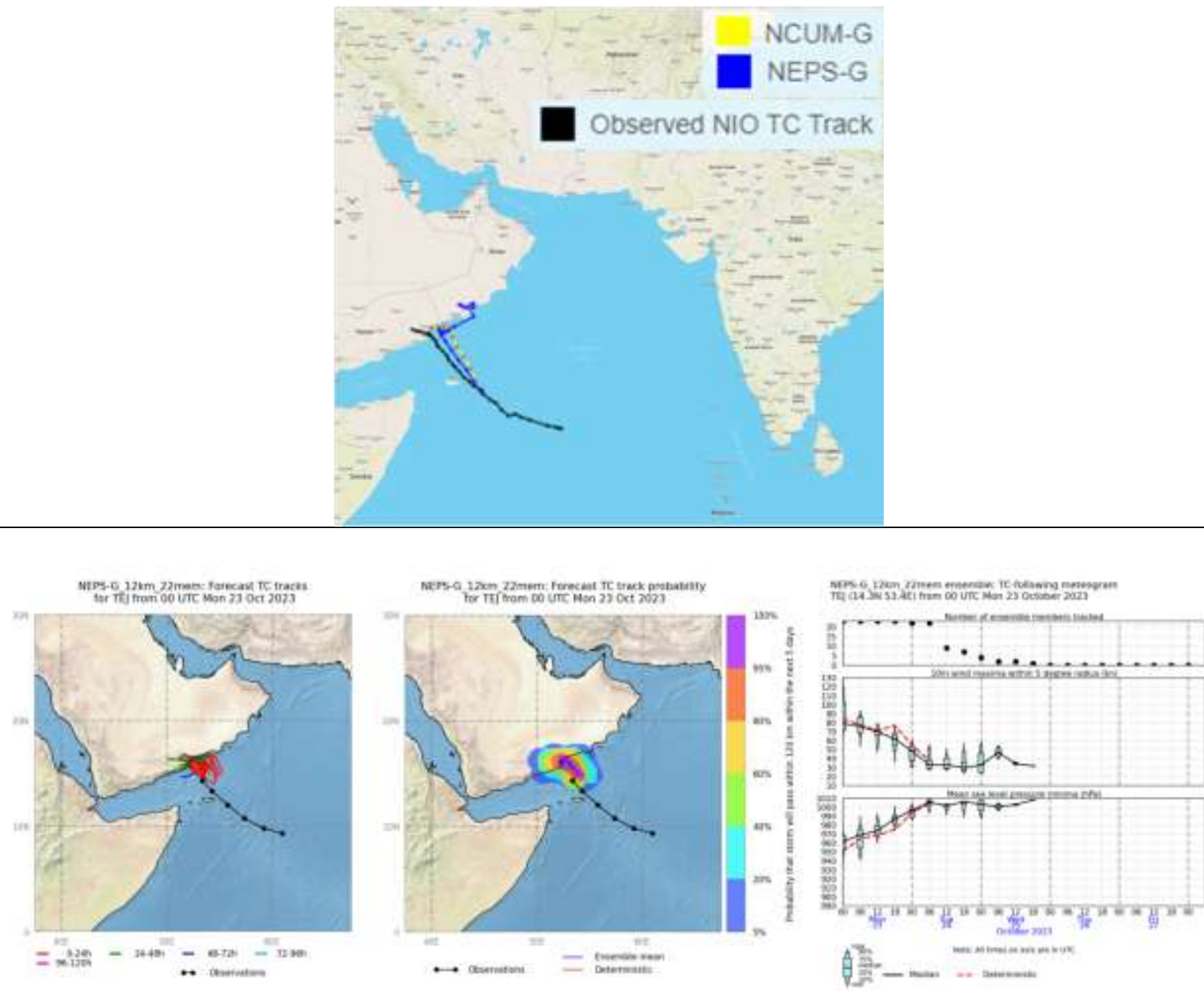

Figure 25. Observed & NCMRWF model forecast tracks of Arabian Sea ESCS ‘Tej’. Ensemble forecast tracks, strike probability and EPSgrams are based on IC 00UTC 23rd Oct 2023.

6.1.2. Forecast Track Errors

The NCUM-G (ICs 20-24 Oct 2023) and NEPS-G (ICs 20-24 Oct 2023) model forecasts (both 00 and 12UTC runs) have been used in the verification. Table 1 summarizes the track errors. *Mean initial position error is low in both models; 23 km & 44km in NCUM-G and NEPS-G (mean) respectively. Similarly, the 48 and 72hr errors are slightly lower in NCUM-G with 131km and 216km as against 144km and 220km in NEPS-G (mean).*

The track error components, Direct Position Error (DPE), Along Track Error (ATE) and Cross Track Error (CTE) are shown in Figure 26. *DPE & ATE are marginally higher in NEPS-G at higher lead times. On the other hand, CTE is larger in NCUM-G*

Table 1. ***Forecast Track Errors NCUM-G and NEPS-G (numbers in the adjacent column in italics indicate number of forecast points validated)***

	DPE			
Fcst. Hour	**NCUM-G**	**No of Forecast verified**	**NEPS-G**	**No of Forecast verified**
0	23	*5*	44	*8*
12	64	*6*	64	*8*
24	83	*8*	73	*7*
36	100	*7*	103	*6*
48	131	*6*	144	*5*
60	166	*5*	182	*4*
72	216	*7*	220	*3*
84	259	*7*	271	*2*
96	277	*6*	323	*1*
108	265	*5*	NA	*0*
120	222	*4*	NA	*0*

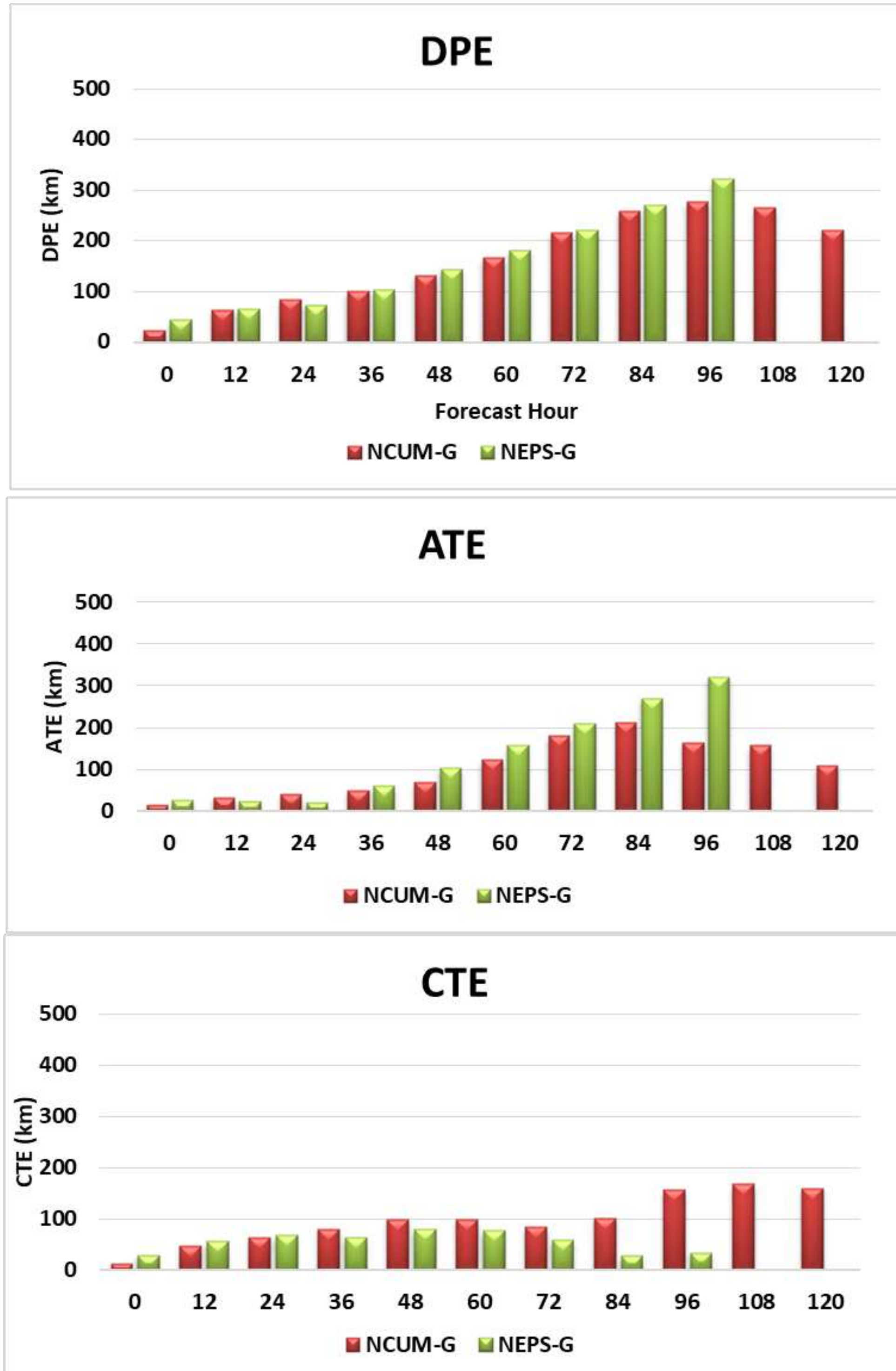

Figure 26. Track forecast errors (top) Direct Position Error (DPE), (middle) Along Track Error (ATE), and (bottom) Cross Track Error (CTE) in km.

6.1.3. Forecast Intensity Errors (Min SLP and Max Wind)

The mean absolute error (MAE) in forecast central pressure (CP)/minimum Sea Level Pressure (min SLP) and maximum sustained wind (MSW) for NCUM-G model is shown in Figure 27. *At the initial time, the MAE in CP<8 hPa is low. However, the MAE in MSW > 10kts can be considered high. In Figure 28 NCUM-G forecasts of CP and MSW show that model has usually underestimation of intensity except on 23rd Oct.*

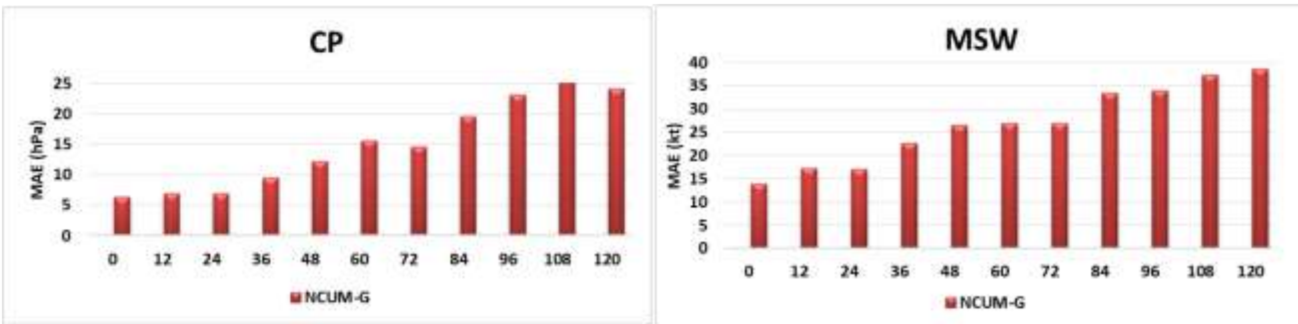

Figure 27. Mean Absolute Error (MEA) in CP (hPa) and MSW (kt) at different forecast lead times.

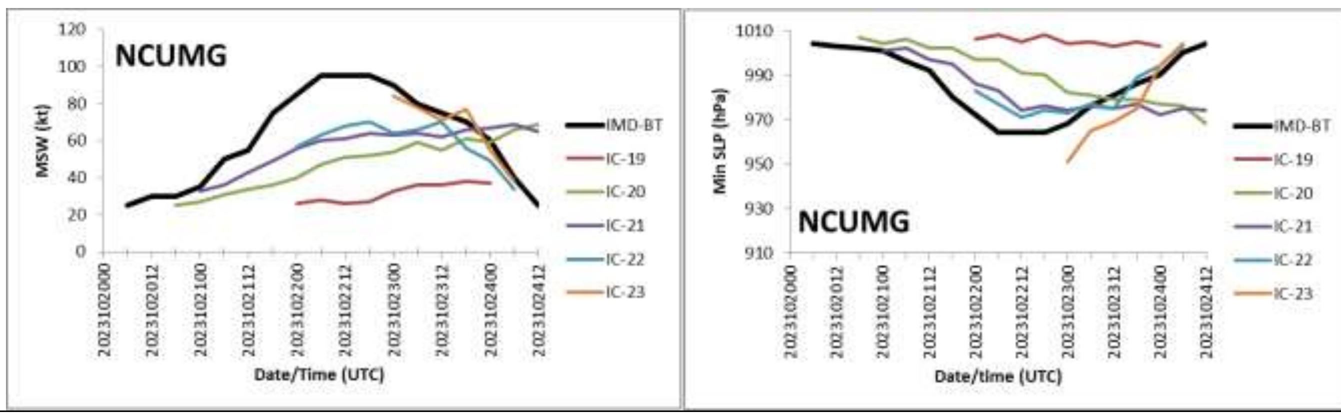

Figure 28. Intensity given by MSW (kt; left) & Min. SLP (hPa; right) in NCUM-G forecasts with different initial conditions from 19th to 23rd Oct 2023. Comparison with observations (BT) is also given.

6.1.4. Forecast Landfall Error

As per the IMDs best track data, the ESCS Taj crossed Yemen coast between (between 21:00 and 22:00 UTC of 23rd October) near 15.90°N/52.15°E with the strength of VSCS. The forecast landfall errors have been computed using the first forecast position on the land. *The forecast landfall time errors in both models are large and positive indicating large delay in predicted land fall time. However, the NCUM-G forecast landfall* *time error after 22nd Oct is low at 6h delay. The landfall position errors are high (> 200km) in both models on 20th Oct 2023 however, in NCUM-G the landfall position errors are low (<50km) from 21st Oct 2023.*

Table 2. ***Error in the forecasted landfall time and position (Forecast time – Observed time) [-ve depicts early landfall and +ve shows delay in landfall]***

	NCUM-G		NEPS-G	
	Position(km)	**Time(hr)**	**Position(km)**	**Time(hr)**
2023102012	250	30	240	30
2023102100	250	30	238	36
2023102112	45	18	166	30
2023102200	45	6	168	36
2023102212	35	6	200	30
2023102300	25	6	20	24
2023102312	NA	NA	10	24

6.1.5. Verification of Strike Probability

Cyclone strike probability is the probability of locating cyclone within 120km of any grid point. Verification of strike probability is presented using Relative Operating Characteristics (ROC) and Reliability diagram (attributes diagrams). It must be noted that the verification of strike probability is presented for a period from 20-24 Oct 2023. The Reliability diagram gives a comparison of forecast probability against the observed frequencies. A perfect match will show all points along the diagonal line. Points above diagonal suggest underestimation (lower forecast probabilities) while points below the diagonal suggest over estimation (higher forecast probabilities).

For the case of ESCS Tej, the verification of strike probability obtained from NEPS-G is carried out using the best track data. Figure 29 shows the reliability and ROC plots for the strike probability verification. In the Reliability diagram, the points along the diagonal indicate the best performing model. While some points below the diagonal indicate overestimation of cyclone strike probability. The ROC curve of NEPS-G shows that the model has skill as the curve is away from the diagonal line of no resolution. The AROC (area under the ROC) is 0.77 which is also indicative of reasonably good resolution in the model.

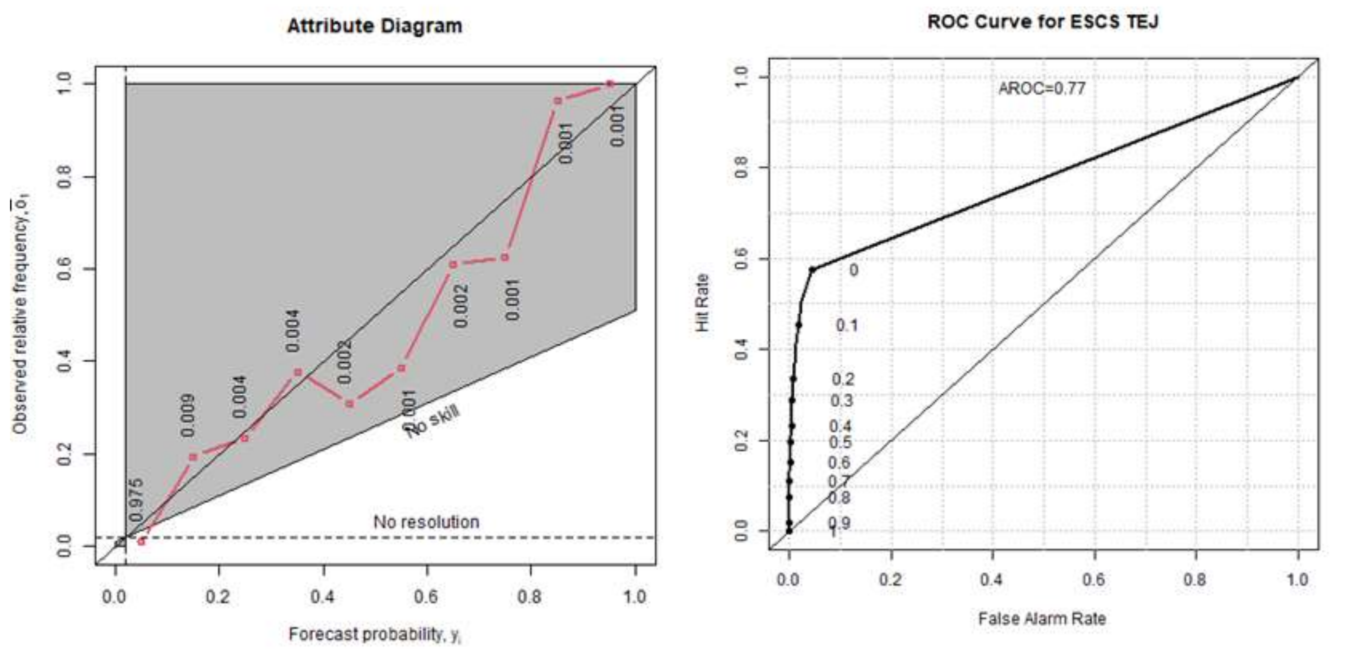

Figure 29. Verification of strike probability using reliability diagram (left) and ROC curve (right) for the case of ESCS 'Tej'.

6.2. Bay of Bengal VSCS ' Hamoon ' during 21-25 Oct 2023

This subsection provides brief summary on the verification of the NCMRWF model forecasts for the recent VSCS 'Hamoon' during 21-25 Oct 2023, which developed over Bay of Bengal (BoB). The VSCS Crossed Bangladesh Coast to the south of Chittagong near (21.900N/91.900E) between 1900 UTC and 2000 UTC of 24th Oct 2023 as an SCS with maximum sustained wind speed of 45 knots and gusting to 55 knots. Verification of the forecasts is presented for NCMRWF Unified Models; NCUM-G (12km grid resolution) and NEPS-G mean (12km grid resolution) and NCUM-R (4 km grid resolution) for both 00UTC and 12UTC runs.

6.2.1. Forecast Tracks and Strike Probability

The observed and model predicted tracks based on 00UTC of 24th Oct 2023 are shown in Figure 30 (top). All the predicted tracks indicated that VSCS 'Hamoon' would track towards Myanmar. For the same initial condition, the strike probability (Figure 30; bottom) based on the 23 (1 control + 22 perturbed) members NEPS-G ensemble also indicate that the cyclone would approach the Myanmar coast.

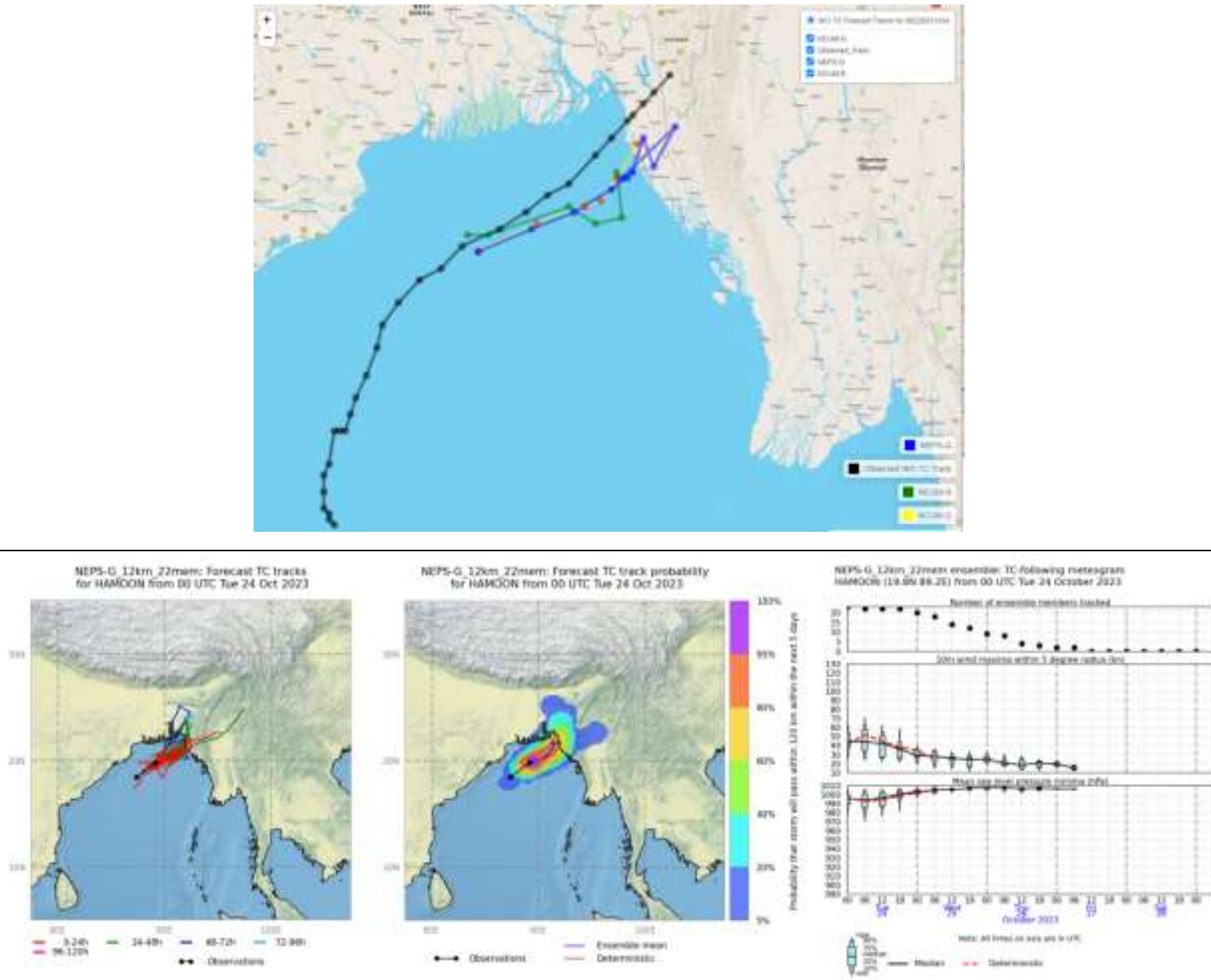

Figure 30. Observed & NCMRWF model forecast tracks of Bay of Bengal VSCS ‘Hamoon’ (top). Ensemble forecast tracks, strike probability and EPSgrams (bottom) are based on IC 00UTC 24th Oct 2023.

6.2.2. Forecast Track Errors

The NCUM-G, NCUM-R (ICs 20-24 Oct 2023), and NEPS-G (ICs 22-25 Oct 2023) model forecasts (both 00 and 12UTC runs) have been used in the verification. Although models are verified at 6 hourly intervals, the results have been presented at 12hr intervals. Table 3 summarizes the track errors for all the models. *Mean initial position error is least (46km) in NEPS-G. The initial error is 55 km & 59km in NCUM-G and NCUM-R respectively. Similarly, the 48 & 72hr errors are lowest in NEPS-G.* The track error components; Direct Position Error (DPE), Along Track Error (ATE) and Cross Track Error (CTE) are shown in Figure 31. *DPE & ATE are marginally higher in NCUM-G. On the other hand, CTE is larger in NCUM-R.*

Table 3. ***Forecast Track Errors NCUM-G and NEPS-G (numbers in the adjacent column in italics indicate number of forecast points validated)***

Fcst Hour	NCUM-R	No of Fcst. verified	NCUM-G	No of Fcst. verified	NEPS-G	No of Fcst. Verified
0	59	*6*	55	*5*	46	*7*
12	61	*7*	74	*5*	78	*6*
24	98	*6*	144	*4*	111	*5*
36	103	*7*	166	*5*	122	*4*
48	151	*7*	168	*4*	112	*3*
60	169	*5*	171	*3*	98	*2*
72	231	*5*	224	*4*	178	*1*
84			331	*3*	NA	*0*
96			340	3	NA	0
108			374	3	NA	0
120			323	2	NA	0

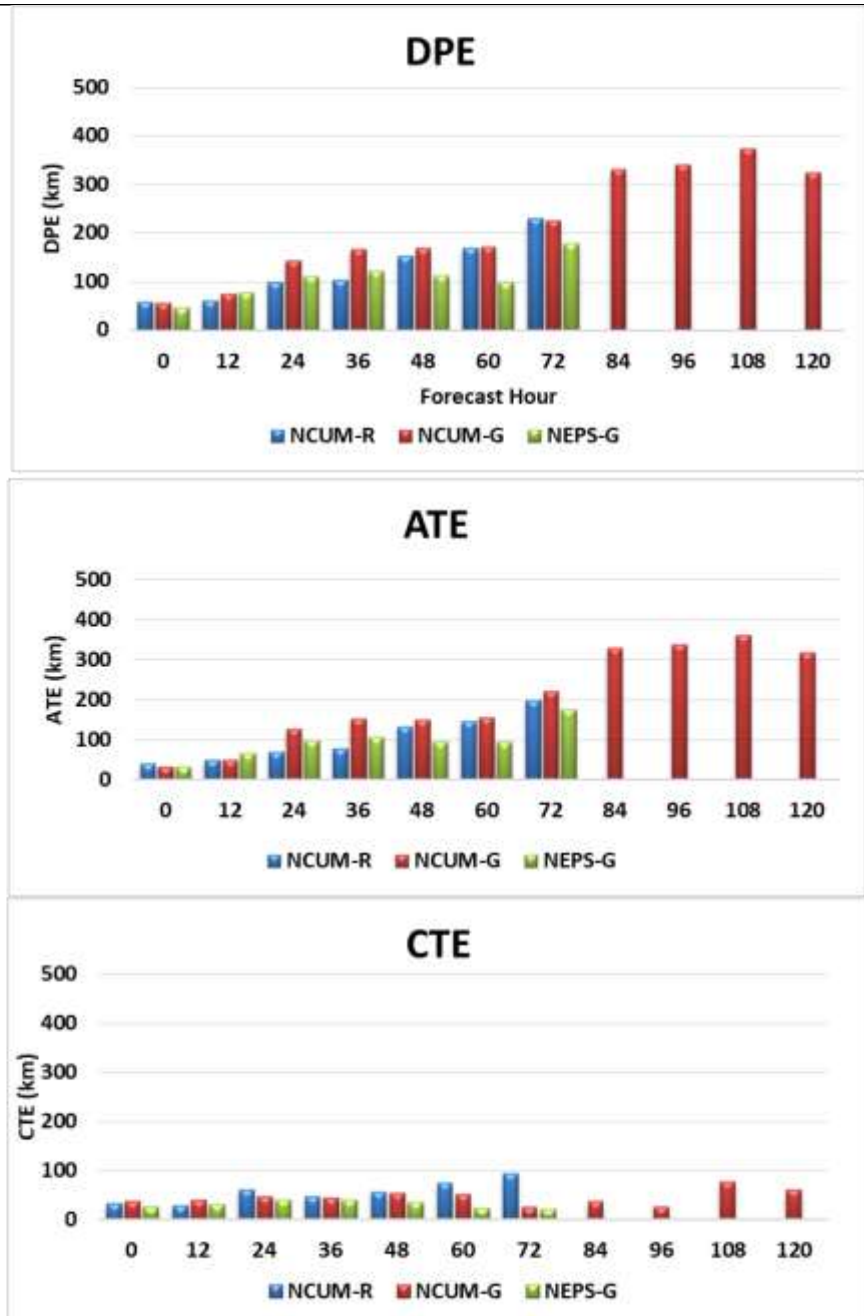

Figure 31. Track forecast errors (a) Direct position error (DPE), (b) Along track error (ATE), and (c) Cross track error (CTE) in km from different models at 12 hourly intervals.

6.2.3. Forecast Intensity Errors (Min SLP and Max Wind)

The mean absolute error (MAE) in forecast of central pressure (CP)/minimum Sea Level Pressure (min SLP) and maximum sustained wind (MSW) for NCUM-R and NCUM-G models are shown in Figure 32. *At the initial time, the MAE in the model predicted intensity is around 5 however, the error is more in NCUM-R predicted MSW (approx. 15 kt). The errors are marginally higher in NCUM-R at 60 and 72h forecast lead* *times.* The intensities for different ICs are presented in Figure 33. NCUM-G shows the underestimation for all ICs whereas NCUM-R predicted intensities are higher during early forecasts (ICs 21 and 22 Oct). NCUM-R has predicted the peak intensity of the system on 22nd Oct but with substantially higher values.

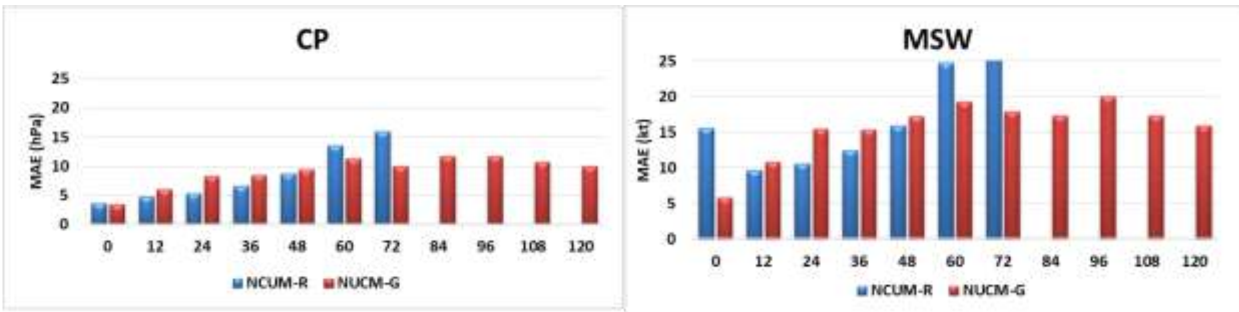

Figure 32. Mean Absolute Error (MEA) in CP (hPa) and MSW (kt) at different forecast lead times.

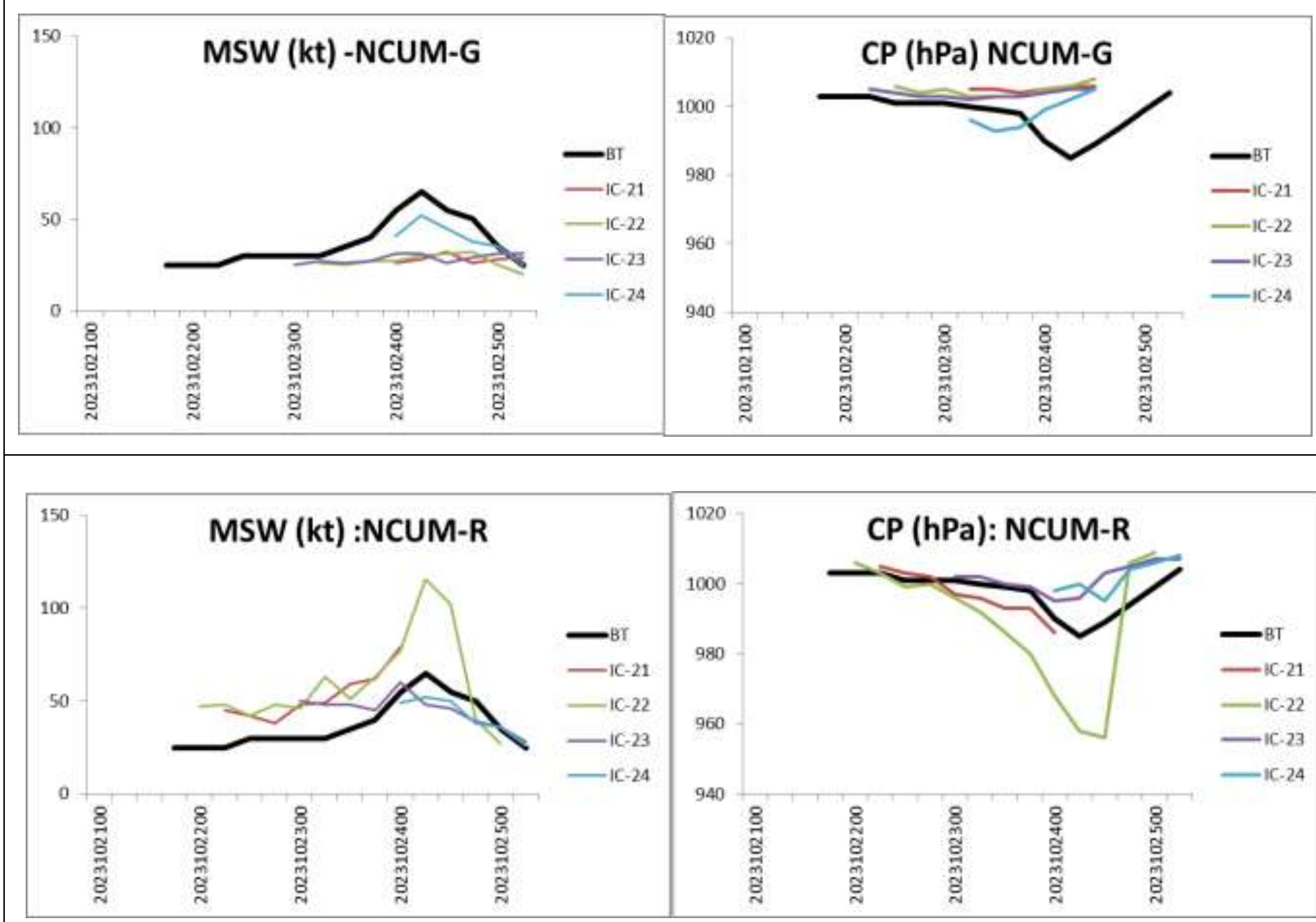

Figure 33. Intensity given by MSW (left) & Min SLP (right) in NCUM-G (top) and NCUM-R (bottom) forecasts with different initial conditions from 19th to 23rd Oct 2023. Comparison with observations (BT) is also given.

6.2.4. Forecast Landfall Error

As per the IMDs best track data the VSCS 'Hamoon' crossed Bangladesh coast to the south of Chittagong near 21.900N/91.900E between 1900 UTC and 2000 UTC of 24th Oct as an SCS with maximum sustained wind speed of 45 knots. NCMRWF global models predicted the model landfall consistently from 22nd Oct whereas the regional model was very uncertain about the system making landfall. The model forecast landfall errors have been computed using the first forecast position on the land. *The forecast landfall time errors in both global models are large and positive indicating large delay in predicted landfall time. However, the NCUM-R forecast error on 00UTC run of 22nd Oct is low with 6h late landfall. The landfall position errors are low (< 120km) in all the models for all the ICs. In NCUM-G the landfall position was very accurate with the error values <20km for the ICs 22nd and 23rd Oct 2023.*

Table 4. ***Error in the forecasted landfall time and position (Forecast time – Observed time) [-ve depicts early landfall and +ve shows delay in landfall]***

	NCUMG		**NCUM-R**		**NEPS-G**	
	Position	Time	Position	Time	Position	Time
2023102100	65	30	NA	NA	NA	NA
2023102112	75	30	NA	NA	NA	NA
2023102200	NA	NA	100	-6	NA	NA
2023102212	15	24	78	-12	60	30
2023102300	0	30	NA	NA	70	30
2023102312	118	30	NA	NA	98	30
2023102400	30	6	NA	NA	70	48
2023102400	35	12	25	6	0	6

6.2.5. Verification of Strike Probability

Cyclone strike probability is the probability of locating cyclone within 120km of any grid point. Verification of strike probability is presented using ROC and Reliability diagram (attributes diagrams). It must be noted that the verification of strike probability is presented for a period from 20-24 Oct 2023. The Reliability diagram gives a comparison of forecast probability against the observed frequencies. A perfect match will show all points along the diagonal line. Points above diagonal suggest underestimation (lower forecast probabilities) while points below the diagonal suggest over estimation (higher forecast probabilities).

For the case of VSCS 'Hamoon', the verification of strike probability obtained from NEPS-G is carried out using the best track data. Figure 34 shows the reliability and ROC plots for the strike probability verification.

In the Reliability diagram, the points along the diagonal indicate best performing model. While some points below the diagonal indicate over estimation of cyclone strike probability. The ROC curve of NEPS-G shows that the model has skill as the curve is away from the diagonal line of no resolution. The AROC (area under the ROC) is 0.84 which is also indicative of good resolution in the model.

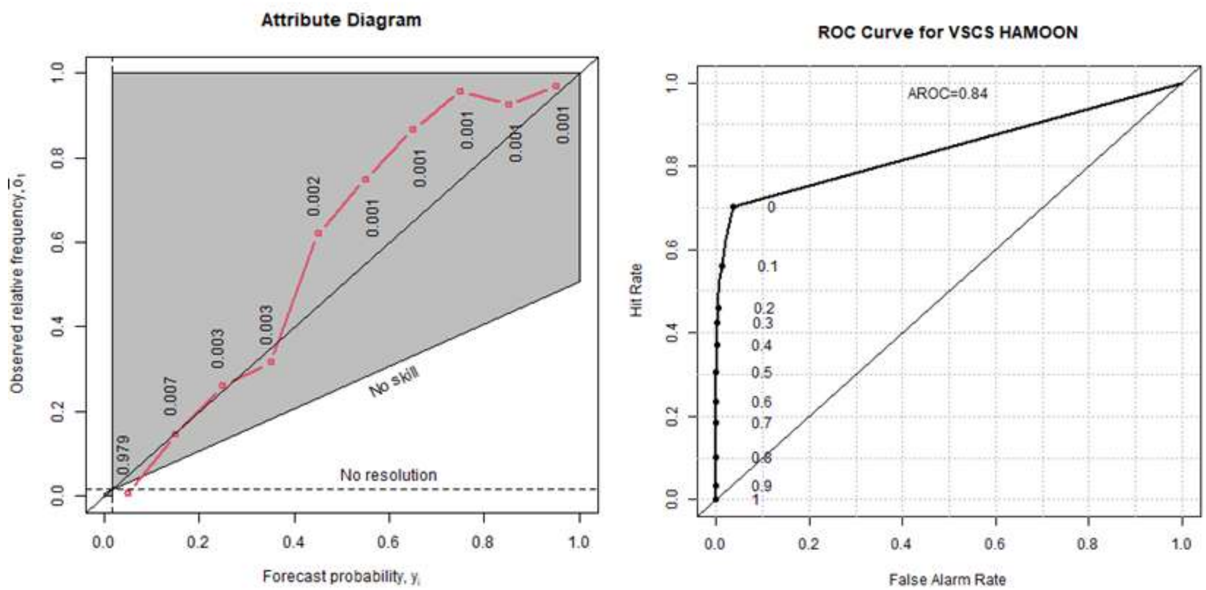

Figure 34. Verification of strike probability using reliability diagram (left) and ROC curve (right) for the case of VSCS 'Hamoon'.

7. Summary and Conclusions

This report documents performance of the NCMRWF model forecasts during winter season ON 2023. The verification results are presented to address both forecasters and model developers. The information on biases in the forecast winds, temperature, humidity, rainfall, etc., are crucial for the forecasters to interpret the model guidance for forecasting. Additionally, information on recent improvements in the model skill adds to confidence in the model forecasts. The results of the study can be summarized below.

7.1. NCUM-G Mean analysis and anomalies during ON 2023

- *The low-level wind anomalies at 850 and 700 hPa levels show the presence of easterly/northeasterly winds indicating the Post-monsoon (ON) over south peninsular India. The ON 2023 anomaly winds show stronger easterlies over the equatorial Indian Ocean. This pattern of anomalies extends up to 500 hPa. At 500 hPa, the deflection of westerlies between 20-40^{0}N and 80-100^{0}E can be seen in the mean winds due to Himalayan topography. The strength for these westerlies has increased at 200 hPa level. The maxima of subtropical jet (STJ) is clearly* *seen at 200 hPa with magnitudes more than 40m/s. The anomalies suggest the weakening of the jet above 25^{0}N and strengthening below 25^{0}N.*

- *Low level (850 hPa) temperature exceeds 19^{0}C over the north-western Indian regions. In contrast to the temperatures at 850 hPa level, temperature distribution is quite homogeneous ranging between 8-10^{0}C, except over the BoB at 700 hPa. This relatively strong heating in the lower troposphere probably enhances the low-level convergence of winds and troughing and subsequently, the cyclogenesis as noted earlier. The temperature anomalies reveal that the above normal temperature over BoB relative to climatological means with magnitudes of 2^{0}C is favorable for convective initiation over BoB. At 700 hPa, positive anomalies are widespread, except for the north-west parts of India. This pattern of anomalies extends up to 200hPa, excluding the region between 35-40^{0}N and 60-100^{0}E at 200hPa.*
- *During ON-2023 season lower tropospheric humidity is larger over the southern peninsula India due to the strong easterly flow from BoB to the Indian subcontinent. Also, the high humidity can be noticed over the equatorial Indian Ocean and Maritime Continent (MC). When we see the anomalous distribution for the ON 2023, the above normal percentage of RH in the lower troposphere to mid-troposphere can be clearly visible over BoB and coastal regions around the south peninsular India.*

7.2. NCUM-G Systematic Errors

- *Systematic errors in winds at 850 hPa from Day-1 forecasts show an easterly wind bias along equator between 80-100^{0}E. A westerly wind bias over the south Arabian Sea around 60^{0}E is seen in Day-1 forecast which is getting enhanced with forecast lead time. An error in low-level winds enhances the area around the equatorial regions and this could be due to the enhanced convective activity during this season. Similar systematic errors in winds are also noticed at 700 hPa level over the Indian region. Interestingly, westerly wind bias is more prominent at 700 hPa level over the equatorial region and central India in Day-3 and Day-5 forecasts. At 500 hPa, errors in winds are relatively small in Day-1 forecasts. The wind bias seen over equatorial regions is enhancing in Day-3 and Day-5 forecasts with westerlies on the west and easterlies on the east indicating active convection around equatorial regions. Systematic errors at 200 hPa level winds show enhanced divergent circulation along the equatorial regions on Day-3 and a similar spatial pattern in winds is also seen on Day-5 with enhanced error magnitudes.*
- *Model shows warm bias (~1^{0}C) occupied over northwestern Indian land mass and over the oceanic regions i.e., AS and BoB, and the magnitude of this bias is increasing over land regions with forecast lead time.* Additionally, the bias over equatorial oceanic regions reverses signs and shows a cold bias, which increases with forecast lead time. *Interesting to see that the bias at 700 hPa over the AS and BoB reverse sign and now exhibits cold bias compared to the 850 hPa level. At 500hPa (200hPa), temperature exhibits warm bias (cold bias) over most of the Indian land mass and surrounding oceanic regions excluding northwestern Indian region and AS (western equatorial Indian Ocean and the region between 50-100^{0}E and 30-45^{0}N), and the magnitude of the bias is increasing in forecasts with lead time. Errors in upper-troposphere (200hPa) temperatures show a large patch of warm bias over the western equatorial Indian Ocean and over the region between 50-100^{0}E and 30-45^{0}N is prominent in Day-3 and Day-5 forecasts.*
- *Systematic errors at 850 hPa level show dry bias over the Indian land region, most of the Indian subcontinent, and regions surrounding MC; and this dryness is enhancing with forecasts lead time, which could possibly influence the MJO propagation through MC in NCUM-G. Interestingly the dry bias seen over Indian subcontinent excluding peninsular India region at 850 hPa level changed sign to positive and moist bias is seen at 700 hPa level. However, the dryness over MC and surrounding regions persists at all the levels from 700 to 200 hPa.*

- ❖ *Systematic errors of winds at 10m show the presence of feeble cyclonic circulation over BoB and south-westerlies over AS and BoB in Day-3 and Day-5.*
- ❖ *Systematic errors show a relatively cold bias (< -1^0C) over Indian land regions* excluding northwestern region *and these cold biases are increasing with forecast lead time. This can be attributed to the presence of arid regions and resulting in large sensible heat flux and dry north-westerly winds from the northwest towards Indian region.*
- ❖ *Systematic error in PWAT shows a column dry over Indian land regions in Day-1, this dryness in column is enhancing with forecast lead time and its magnitude is maximum on Day-5. Large positive (negative) PWAT biases are seen over the AS and equatorial (MC) regions. This excess (deficit) column water on the equatorial regions will influence the MJO convection and propagation towards the west Pacific.*

7.3. Rainfall Forecast Verification

- ❖ *NCUM-G forecast overestimates post-monsoon mean rainfall amounts over the north-eastern regions, BOB, and the oceanic regions around the equator. Apart from this, most of the Indian subcontinent is dry with no convection in both observations and forecasts. Small dry bias regions are noticed over Sri Lanka, Bangladesh, and some parts of Tamil Nadu. In contrast, wet bias (blue) over southern parts of the oceanic regions is seen.*
- ❖ *For different rainfall thresholds, POD and FAR show decrease and increase in scores, respectively. The BIAS score (frequency bias) indicates that forecasts overestimate the frequency up to 9mm/day thresholds. The values of PSS and SEDI, all are high for rainfall up to 9 mm/day suggesting reasonable skill. PSS score shows a very sharp decrease as the threshold varies. Overall, the skill is not bias-free. For higher rainfall thresholds (> 10 mm/day), frequency bias is almost constant, but the skill is low as indicated by CSI, PSS, and SEDI.*

7.4. Significant Weather Features during ON 2023

❖ Arabian Sea ESCS 'Tej' during 20-24 Oct 2023

- ➢ ***Initial Position Erro**r: Mean initial position error is low in both models; 23 km & 44km in NCUM-G and NEPS-G (mean) respectively.*
- ➢ ***Direct Position Erro**r: 48 and 72 hr errors are slightly lower in NCUM-G with 131km and 216km as against 144km and 220km in NEPS-G (mean). DPE & ATE are marginally higher in NEPS-G at higher lead times, CTE is larger in NCUM-G*
- ➢ ***Landfall Position & Time error**: The forecast landfall time errors in both models are large and positive indicating large delay in predicted landfall time. However, the NCUM-G forecast landfall time error after 22nd Oct is low at 6h delay. The landfall position errors are high (> 200km) in both models on 20th Oct 2023. In NCUM-G the landfall position error is low (<50km) from 21st Oct 2023.*
- ➢ ***Intensity verification (NCUM-G)**: At the initial time, the MAE in CP<8 hPa is low. However, the MAE in MSW > 10kts can be considered high.*
- ➢ ***Verification of strike probability (NEPS-G)**: ROC and Reliability diagrams are used for this purpose. The NEPS-G model is over forecasting. The ROC curves show that the models have reasonable skill (AROC is 0.77).*

❖ Bay of Bengal VSCS ' Hamoon ' during 21-25 Oct 2023

- ***Initial Position Erro**r: Mean initial position error is least (46km) in NEPS-G. The initial error is 55 km & 59km in NCUM-G and NCUM-R respectively.*
- ***DPE, ATE, and CTE**: DPE & ATE are marginally higher in NCUM-G. On the other hand, CTE is larger in NCUM-R.*
- ***Landfall Position & Time error**: The landfall position errors are low (< 120km) in all the models for all the ICs. In NCUM-G the landfall position was very accurate with the error values <20km for the ICs 22nd and 23rd Oct 2023.*
- ***Intensity verification (NCUM-G)**: At the initial time, the MAE in the model predicted intensity is around 5 however, the error is more in NCUM-R predicted MSW (approx. 15 kt).*
- ***Verification of strike probability (NEPS-G)**: ROC and Reliability diagrams are used for this purpose. The NEPS-G model is under-forecasting. The ROC curves show that the models have reasonable skill (AROC is 0.84).*

References

1. Ashrit R, Sharma K, Dube A, Iyengar G R, Mitra A K and Rajagopal E N 2015b: Verification of short-range forecasts of extreme rainfall during monsoon; Mausam 66 375–386, 607.
2. Barker, D., 2011. Data assimilation-progress and plans, MOSAC-16, 9-11 November 2011, Paper16.6.
3. Hersbach H, Bell B, Berrisford P, et al. 2020: The ERA5 global reanalysis. Q J R Meteorol Soc. 2020;146:1999–2049. https://doi.org/10.1002/qj.3803
4. Jolliffe, I. T., and D. Stephenson, 2012: Forecast Verification: A Practitioner's Guide in Atmospheric Science, John Wiley & Sons, Ltd.
5. Kumar Sumit, A. Jayakumar, M. T. Bushair, Buddhi Prakash J., Gibies George, Abhishek Lodh, S. Indira Rani, Saji Mohandas, John P. George and E. N. Rajagopal 2018: Implementation of New High Resolution NCUM Analysis-Forecast System in Mihir HPCS. NMRF/TR/01/2019, 17p.
6. Kumar Sumit, M. T. Bushair, Buddhi Prakash J., Abhishek Lodh, Priti Sharma, Gibies George, S. Indira Rani, John P. George, A. Jayakumar, Saji Mohandas, Sushant Kumar, Kuldeep Sharma, S. Karunasagar, and E. N. Rajagopal 2020: NCUM Global NWP System: Version 6 (NCUM-G:V6), NMRF/TR/06/2020.
7. Kumar Sumit, Gibies George, Buddhi Prakash J., M. T. Bushair, S. Indira Rani and John P. George 2021: NCUM Global DA System: Highlights of the 2021 upgrade, NMRF/TR/05/2021.
8. M. Rajeevan, C.K. Unnikrishnan, J. Bhate, K. Niranjan Kumar, P.P. Sreekala Northeast monsoon over India: variability and prediction Met. Apps, 19 (2012), pp. 226-236
9. Mitra, A. K., A. K. Bohra, M. N. Rajeevan and T. N. Krishnamurti, 2009: Daily Indian precipitation analyses formed from a merged of rain-gauge with TRMM TMPA satellite derived rainfall estimates, J. of Met. Soc. of Japan, 87A, 265-279.
10. Mitra, A. K., I. M. Momin, E. N. Rajagopal, S. Basu, M. N. Rajeevan and T. N. Krishnamurti, 2013, Gridded Daily Indian Monsoon Rainfall for 14 Seasons: Merged TRMM and IMD Gauge Analyzed Values, J. of Earth System Science, 122(5), 1173-1182.
11. Sharma, K., Ashrit, R., Kumar, S. et al. Unified model rainfall forecasts over India during 2007–2018: Evaluating extreme rains over hilly regions. J Earth Syst Sci 130, 82 (2021). https://doi.org/10.1007/s12040-021-01595-1
12. Srivastava A K, Rajeevan M and Kshirsagar S R 2009: Development of a high resolution daily gridded temperature data set (1969–2005) for the Indian region; Atmos. Sci. Lett. 10 249–254, https://doi.org/10.1002/asl.232
13. Stephenson D.B., B. Casati, C.A.T. Ferro and C.A. Wilson, 2008: The extreme dependency score: a non-vanishing measure for forecasts of rare events. Meteorol. Appl., 15, 41-50.
14. Walters, D., and co-authors: The Met Office Unified Model Global Atmosphere 6.0/6.1 and JULES Global Land 6.0/6.1 configurations, Geosci. Model Dev., 10, 1487–1520, https://doi.org/10.5194/gmd-10-1487-2017, 2017.
15. Wilks D S 2011 (eds) Statistical methods in the atmospheric 807 sciences; 3rd edn, Elsevier, 676p